Unclassified

5 p. GO

NASA CR-50943

MASSACHUSETTS INSTITUTE OF TECHNOLOGY

N63 21481

LINCOLN LABORATORY

CODE-1

AP-17

(Apollo)

EARTH-ORBITAL TRAJECTORY ESTIMATING CAPABILITY OF A SINGLE GROUND RADAR AS FUNCTION OF ITS ANGULAR ACCURACY

5187000

Juris Šlesers

OTS PRICE

XEROX $ [illegible]

MICROFILM $ [illegible]

This document has not been reviewed by the Public Information Office, National Aeronautics and Space Administration, and is therefore not intended for public release. Further dissemination or reproduction in whole or in part of the material within this document shall not be made without the express written approval of Lincoln Laboratory (Publications Office).

5 November 1962 51 p. refs

The work reported in this document was performed at Lincoln Laboratory, a center for research operated by Massachusetts Institute of Technology; this work was supported by the U.S. National Aeronautics and Space Administration under Contract NAS9-105. (NASA

LEXINGTON MASSACHUSETTS

to an ... request made to the ... Department and obtained through direct acquisition.

Unclassified

TABLE OF CONTENTS

Abstract

21431

This paper reports on an investigation of the role and effect of azimuth and elevation measuring capability of a single ground-based radar on the radar's ability to estimate the trajectory of a vehicle in a nominally 100 n. m. circular orbit about a non-rotating spherical earth. The radars measuring range, azimuth, elevation, and range-rate are considered.

This investigation is part of a broader study of trajectory estimation errors.

Introduction

Tracking radars capable of measuring range, range-rate, azimuth, and elevation of a space vehicle have been recommended for the Apollo ground network. A study of the capability of such a network of radar sites to estimate the trajectory of an earth-orbital vehicle entails analysis of the separate and combined effects of a number of variables on the trajectory estimating capability. The present paper is confined to the effects of angular measurement errors as the prime variable.

The Model

The idealized model used in the present analysis embodies the following assumptions:

a. The vehicle is in a thrust-free, drag-free Keplerian orbit in a perfectly known central force field. (Gravitational coefficient = 2.259×10^8 n.m.^{3}/min.^{2}).

b. The earth is spherical (Radius = 3440 n.m.).

c. The earth is non-rotating*.

d. Line-of-sight tracking takes place at all times when the vehicle is at an elevation of not less than 8^o relative to the radar site, and it is free of atmospheric effects. No tracking takes place at elevation of less than 8^o.

e. The radar site is located at sea level.

f. Radar measurement errors in each of the four components measured (i.e., range, azimuth, elevation, range-rate) are normally distributed random variables about a zero mean, and independent for each measurement in each component.

---

* This assumption makes the analysis independent of the relationship of the orbital plane and the site location to the earth's equator. Evaluation of its effect on the results in representative situations has shown this effect to be small (not more than a few percent of the magnitudes of the errors of estimation).

g. Radar measurement errors have known constant variances, independent of the magnitude of the quantity measures.

h. Location and orientation of the radar site is known perfectly*.

Situations Considered: The Geometry

The present analysis considers only nominal trajectories that are circular and 100 n.m. above the earth's surface. Figures 1 and 2 illustrate the geometry of the situations studies.

Figure 1 is a sketch of a vertical section passing through the radar site location. In this figure H stands for "horizon," and LLE means "lower limit on elevation." Hence, the shaded portion which is bounded by the LLE = 8° line represents the region where no tracking can take place. Undisturbed tracking takes place in the unshaded region above LLE = 8°.

Horizontal distances are generally expressed in terms of "earth central angle," (ECA). It is seen that at 100 n.m. altitude a vehicle theoretically must pass the radar site within a maximum distance of 7.78° ECA (467 n.m. measured along the surface) in order to be "visible" to the radar. Computations are carried out for nominal orbits passing the radar site at 0° ECA, 4° ECA, and 7° ECA, respectively, as indicated in Figure 1.

Figure 2 is a horizontal projection of the coverage area and the three nominal trajectories, with the total tracking times indicated**. The vehicle moves at a nominal orbital speed of 252.61 n.m./min., which is equivalent to 4.091° ECA/min.

---

* It is exceptionally important to bear this particular factor in mind whenever an attempt is made to apply the results of this work to specific practical situations, where sizable bias errors may be present.

** Tracking times rounded off to the nearest quarter minute are used, for reasons of practical nature regarding the computer program used. For our model, the true tracking times (computed using plane trigonometry in a horizontal plane) would be:

Proximity of Pass	Tracked Segment of Path	Tracking Time
0° ECA	15.57° ECA	3.81 min.
4° ECA	13.38° ECA	3.27 min.
7° ECA	6.82° ECA	1.67 min.

1° ECA = 60 n.m. surface measure.

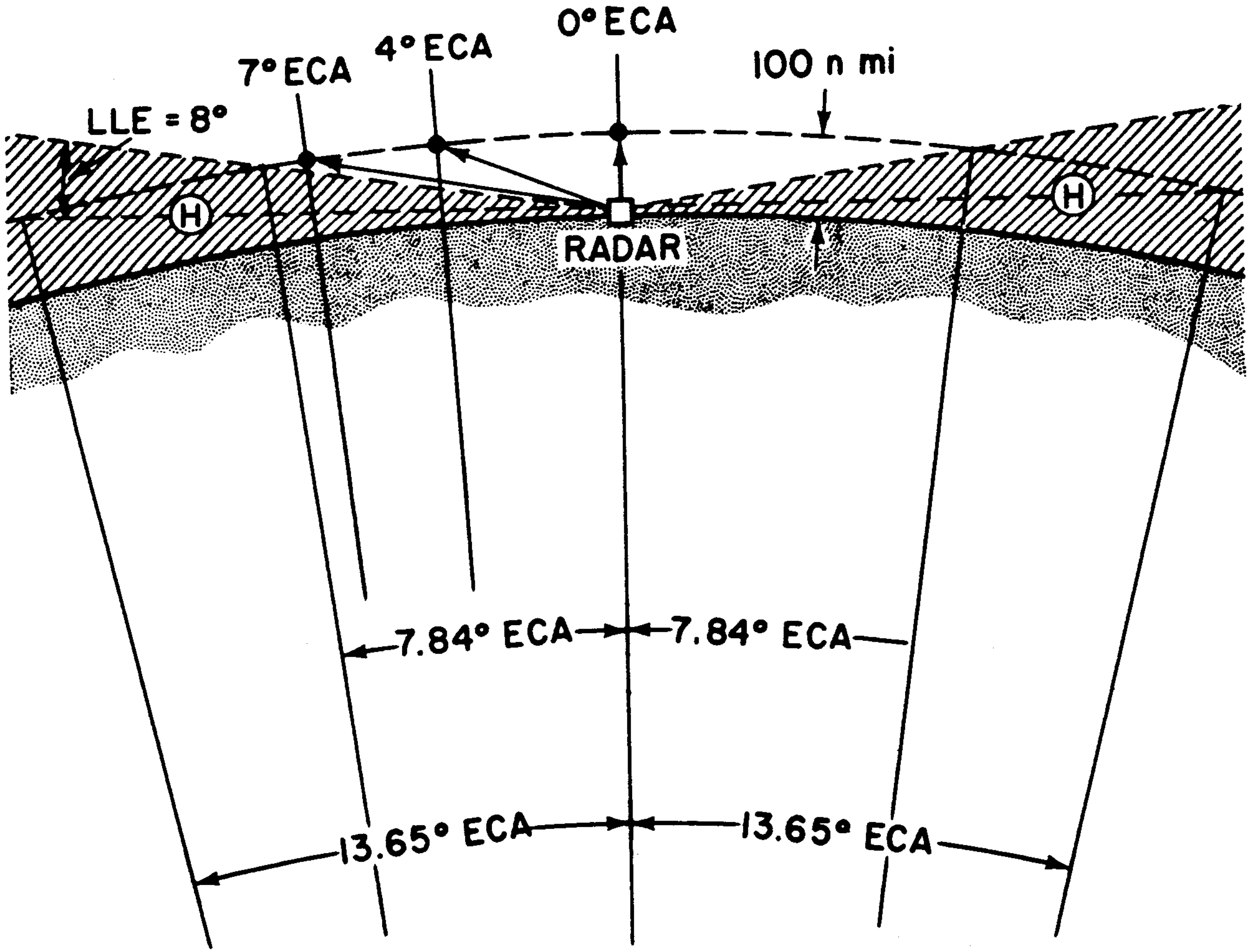

SITUATIONS CONSIDERED: THE GEOMETRY
VERTICAL SECTION, NORMAL TO TRAJECTORY

C28-62

Fig. 1

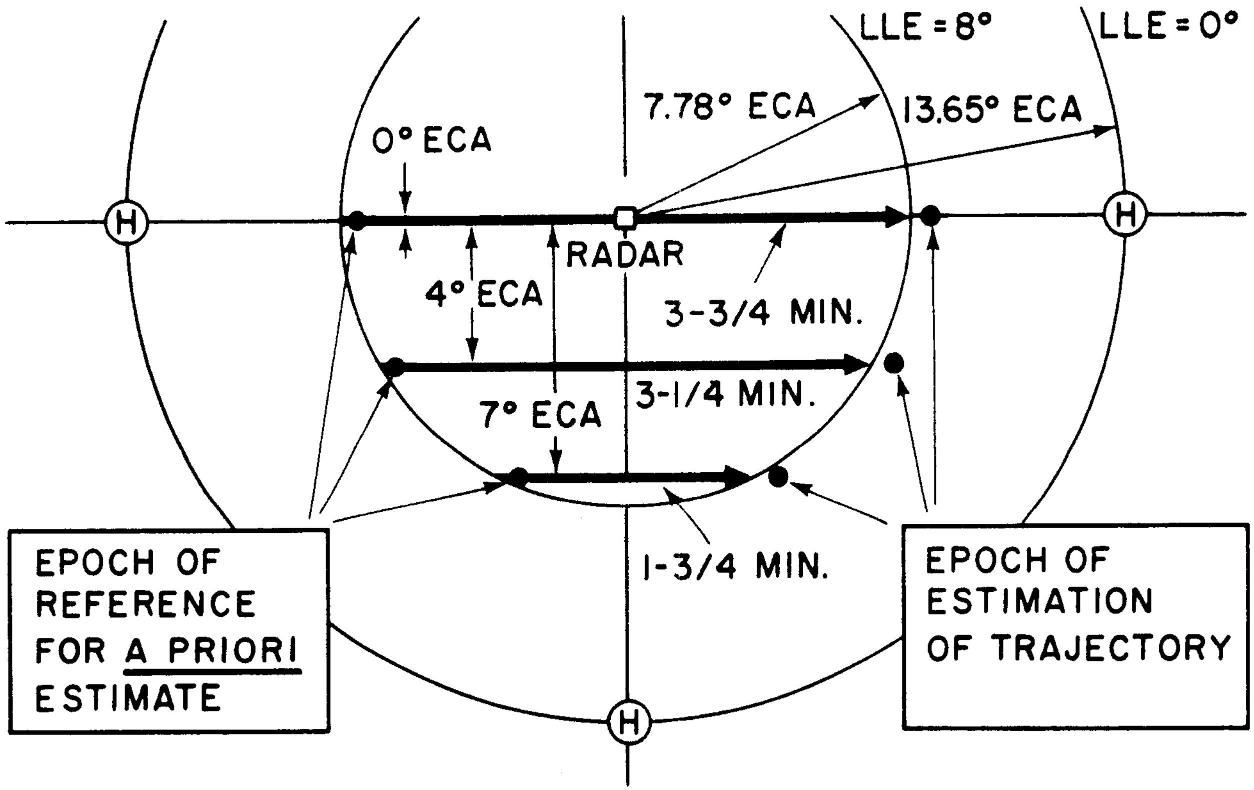

1° ECA = 60 n mi ON THE SURFACE
ORBITAL SPEED = 4.091° ECA / MINUTE

SITUATIONS CONSIDERED: THE GEOMETRY HORIZONTAL PROJECTION

Fig. 2

The trajectory estimation errors in all cases are computed for that epoch in the nominal trajectory which lies just beyond termination of tracking. These epochs are indicated by markers in Figure 2.

The following table lists the tracking times and epochs of estimation (measured from commencement of tracking), used in the present study:

Proximity of Pass	Tracking Time	Epoch of Estimation
0° ECA	3-3/4 min.	3-7/8 min.
4° ECA	3-1/4 min.	3-3/8 min.
7° ECA	1-3/4 min.	1-7/8 min.

In those situations where a priori trajectory information from another source (in addition to the tracking data from the radar site under consideration) is introduced into the computation of the trajectory estimate, this a priori information is given in terms of that epoch of the nominal trajectory 1/8 min. following commencement of tracking. These epochs are also indicated by markers in Figure 2.

Situations Considered: The Radar

The basic radar considered in the computations has expected measurement errors in range and range-rate*:

$$\sigma_R = 10 \text{ ft.}$$

$$\sigma_{\dot{R}} = .5 \text{ ft./sec.},$$

and is capable of making statistically independent measurements of range, range-rate, azimuth, and elevation at the rate of 10 measurements per second. (The measurement errors in each of the 4 components measured at any one epoch are also independent of one another.)

---

* All errors (errors of estimation as well as errors of measurement) in this study are specified as the standard deviation of a normally distributed random variable with a zero mean.

The standard deviation of the measurement errors in elevation is of the same magnitude as that in azimuth. This quantity, σ_A, is the prime input variable in the present analysis. For the basic values of range and range-rate errors, σ_A is varied over the range of .005 to 5 milliradians in steps of one-half order of magnitude*.

Through a simple scaling procedure, it is possible to scale the computed estimation errors for the above family of radar characteristics to any number of related families, differing from the basic one by a common factor in all the error terms. For example, multiplication of the computed estimation error terms for the above family of radars by 10, yields us the corresponding estimation error terms for the following related family of radars:

$$\sigma_R = 100 \text{ ft.}$$

$$\sigma_{\dot{R}} = 5 \text{ ft./sec.}$$

$$\sigma_A = .05 \text{ to } 50 \text{ milliradians.}$$

Or, through multiplication of all error terms by 1/10, we obtain the computed estimation errors for:

$$\sigma_R = 1 \text{ ft.}$$

$$\sigma_{\dot{R}} = .05 \text{ ft./sec.}$$

$$\sigma_A = .0005 \text{ to } .5 \text{ milliradians.}$$

The justification for the above procedure lies in the fact that when deviations from the nominal orbit are small compared to the orbital velocity and radius, the equations of motion may be reduced, for the purpose of computing partial derivations, to a set of linear equations. This means that the relationship between the measurement and estimation errors is effectively a linear one for small deviations. This has been found to be valid for estimation errors as large as 30,000 ft. in position and 200 ft./sec. in velocity. The design of the computer program used in the computations is based on this linearity principle.

---

* I.e., σ_A = .005, .016, .05, .16, etc.

There exists also an equally simple procedure to scale these computations to radars whose sampling rate differs from the 10 measurements per second rate chosen for the basic radar. This is due to the fact that, for sufficiently high sampling rates, the quantities measured by the radar do not change appreciably during the interval between successive sampling epochs and can be "smoothed" over a number of sampling intervals. Varying the radar's expected measurement errors in all components in direct proportion to the square root of the sampling rate leaves the trajectory estimation errors unchanged*, **. Thus the estimation error computations for a radar with measurement errors as given in Column A below, at 10 measurements per second, are equally valid for a radar having the characteristics given in Column B, operating at 1 measurement per second***.

A - 10 meas. /sec.	B - 1 meas. /sec.
σ_R = 100 ft. $\sigma_{\dot{R}}$ = 5 ft. /sec. σ_A = .05 to 50 millirad.	σ_R = 30 ft. $\sigma_{\dot{R}}$ = 1.6 ft. /sec. σ_A = .016 to 16 millirad.
σ_R = 10 ft. $\sigma_{\dot{R}}$ = .5 ft. /sec. σ_A = .005 to 5 millirad.	σ_R = 3 ft. $\sigma_{\dot{R}}$ = .16 ft. /sec. σ_A = .0016 to 1.6 millirad.
σ_R = 1 ft. $\sigma_{\dot{R}}$ = .05 ft. /sec. σ_A = .0005 to .5 millirad.	σ_R = .3 ft. $\sigma_{\dot{R}}$ = .016 ft. /sec. σ_A = .00016 to .16 millirad.

* The variance of an estimate is inversely proportional to the number of measurements taken.

** By virtue of both of the above considerations, if the sampling rate is varied but the measurement errors remain statistically constant, the standard deviations of the estimate will vary inversely as the square root of the sampling rate (provided, of course, that the estimate is based entirely on the tracking data from the radar site, and no "outside" sources of information are utilized).

*** One should not be oblivious to the fact that several of the ranges of values shown in this table reach considerably out of the realm of the practically meaningful, and are of entirely academic interest.

Situations Considered: A Priori Information

In addition to "pure" single-radar situations*, as described above, some situations with "a priori" information are also considered; that is, situations are studied where the trajectory of the vehicle with a specified amount of uncertainty, or error, is known independently of the radar measurements.

In the work covered by this paper, a restricted type of a priori information has been considered. It assumes that the trajectory is known equally well in all directions of position and velocity at the "epoch of reference for a priori estimate" (see Fig. 2) which is the commencement of tracking. The ratio of position uncertainty to velocity uncertainty is 1/10 minute or 6 seconds in all cases.

The graphical expositions in this paper contain data on a priori uncertainties of the following magnitudes:

a. 250 ft. and 40 ft/sec in all directions,

b. 25 ft. and 4 ft/sec in all directions.

The General Nature of Estimation Errors

For the idealized model of analysis as described earlier, the expected error of estimation of a trajectory, is completely described by a symmetrical 6×6 covariance matrix, at any specified time, in the six-dimensional space of position and velocity deviations. The same information can, in general, be equally well represented by either the 6×6 covariance matrix or by its inverse matrix, called the "information matrix."** The information matrix, although in many respects the more basic concept of the two, lacks the "meaningfulness," in a human sense, that the covariance matrix possesses.

---

* See subsequent sections entitled, "Measurements to Estimates" and "Results: Discussion," for qualifying remarks regarding the necessity of some a priori knowledge also in these so-called "pure" single-radar situations.

** There are situations where no 6×6 covariance matrix exists, even though the 6×6 information does exist. This occurs when the information matrix is singular. The singular information matrix does, nevertheless, contain valid information about the trajectory estimation uncertainties.

COVARIANCE MATRIX OF ESTIMATION ERRORS

3 × 3
POSITION
COVARIANCE
SUBMATRIX

$$
\left[\begin{array}{ccc|ccc}
\epsilon_x^2 & \cdot & \cdot & \cdot & \cdot & \cdot \\
\mu_{xy} & \epsilon_y^2 & \cdot & \cdot & \cdot & \cdot \\
\mu_{xz} & \mu_{yz} & \epsilon_z^2 & \cdot & \cdot & \cdot \\
\hline
\mu_{x\dot{x}} & \mu_{y\dot{x}} & \mu_{z\dot{x}} & \epsilon_{\dot{x}}^2 & \cdot & \cdot \\
\mu_{x\dot{y}} & \mu_{y\dot{y}} & \mu_{z\dot{y}} & \mu_{\dot{x}\dot{y}} & \epsilon_{\dot{y}}^2 & \cdot \\
\mu_{x\dot{z}} & \mu_{y\dot{z}} & \mu_{z\dot{z}} & \mu_{\dot{x}\dot{z}} & \mu_{\dot{y}\dot{z}} & \epsilon_{\dot{z}}^2
\end{array}\right]
$$

3 × 3
VELOCITY
COVARIANCE
SUBMATRIX

C28-70

Fig. 3

The covariance matrix describes the size, shape, and orientation of the six-dimensional error ellipsoid in the six-dimensional space of position and velocity deviations. The upper left-hand and the lower right-hand 3×3 submatrices of the total covariance matrix describe the three-dimensional position and the velocity error ellipsoids, respectively.

Furthermore, each of the six diagonal terms of the covariance matrix is the variance (standard deviation squared) along the corresponding axis in the chosen coordinate system. The off-diagonal (covariance) terms indicate the amount of correlation between the errors in any two components.

Whereas the terms of the covariance and information matrices are a function of the coordinate system and the orientation of the axes, there are certain quantities characteristic of each matrix which are independent of the coordinate system and orientation*. These are:

t_p, T_p**	-	The trace*** of the 3×3 position-covariance, or position-information, submatrix.
t_v, T_v	-	The trace of the 3×3 velocity-covariance, or velocity-information, submatrix.
d_p, D_p	-	The determinant of the 3×3 position-covariance, or position-information, submatrix.
d_v, D_v	-	The determinant of the 3×3 velocity-covariance, or velocity-information, submatrix.

---

* Here we refer to the 3-dimensional coordinate systems of position deviations and of velocity deviations, and are assuming that the type and orientation of these two coordinate systems are always chosen identical.

** The lower-case letter refers here to the covariance matrix and the upper-case letter to the information matrix.

*** The trace of a symmetrical q×q matrix is the sum of the q diagonal terms.

d, D - The determinant of the total 6×6 matrix*, **.

Trajectory estimation errors, assumed to be normally distributed random variables with zero mean, may be thought of in terms of "error ellipsoids." By an "error ellipsoid" we mean a surface of constant probability density, which for normally distributed random errors is an ellipsoid. For random variable (error vector) of q degrees of freedom,

---

* Certain simple relationships exist between the determinants and sub-determinants of the 6×6 information and covariance matrices:

$$d_p = D_v/D$$

$$d_v = D_p/D$$

$$d = 1/D \ .$$

Also, the following inequalities exist:

$$(T_p/3)^3 \geq D_p, \ (T_v/3)^3 \geq D_v, \ (t_p/3)^3 \geq d_p, \ (t_v/3)^3 \geq d_v \ ;$$

$$D_p D_v \geq D, \ d_p d_v \geq d \ .$$

** To this list may be added the eigenvalues of both 6×6 matrices and the 3×3 position and velocity covariance and information submatrices The eigenvalues, however, have not been utilized in the presently reported work, as the relative difficulty of computing them (i. e., in terms of computer time) seems to outweigh their usefulness.

there exists a family of concentric and geometrically similar error ellipsoids in a q-dimensional error space, and it is described by its q×q covariance matrix. The matrix equation of this family of surfaces is*:

$$\{x_j\} \ \{\mu_{ij}\}^{-1} \ \{x_i\} = \xi^2 \tag{1}$$

$$i = 1, 2, \ldots, q \quad \text{(rows)}$$

$$j = 1, 2, \ldots, q \quad \text{(columns)}$$

In the present case, we are dealing with error vectors of six degrees of freedom, and could, in principle, talk in terms of a six-dimensional error ellipsoid of hybrid (ft. and ft/sec.) dimensions. However, aside from a brief qualitative statement in a later section, no use is made of that concept. Instead, consider the three-dimensional error ellipsoids

---

* $\{x_j\}$ is a 1×q row matrix of the q components of the random variable; $\{x_i\}$ is $\{x_j\}$ transposed, i.e., the q×1 column matrix of the q components of the random variable; $\{\mu_{ij}\}^{-1}$ is the inverse of the q×q covariance matrix; ξ^2 is a parameter which specifies a particular ellipsoid in the family of concentric ellipsoids. Reference: Harold Cramér, Mathematical Methods of Statistics, Princeton Univ. Press, 1946, p. 120, eq. 11.12.3.

defined by the 3×3 covariance submatrix of position (having dimensions in feet) and the corresponding similarly obtained three-dimensional velocity ellipsoids (having dimensions in feet/second)*:

$$[x\ y\ z] \begin{bmatrix} \epsilon_x^2 & \mu_{yx} & \mu_{zx} \\ \mu_{xy} & \epsilon_y^2 & \mu_{zy} \\ \mu_{xz} & \mu_{yz} & \epsilon_z^2 \end{bmatrix}^{-1} \begin{bmatrix} x \\ y \\ z \end{bmatrix} = \zeta^2 \tag{2}$$

$$[\dot{x}\ \dot{y}\ \dot{z}] \begin{bmatrix} \epsilon_{\dot{x}}^2 & \mu_{\dot{y}\dot{x}} & \mu_{\dot{z}\dot{x}} \\ \mu_{\dot{x}\dot{y}} & \epsilon_{\dot{y}}^2 & \mu_{\dot{z}\dot{y}} \\ \mu_{\dot{x}\dot{z}} & \mu_{\dot{y}\dot{z}} & \epsilon_{\dot{z}}^2 \end{bmatrix}^{-1} \begin{bmatrix} \dot{x} \\ \dot{y} \\ \dot{z} \end{bmatrix} = \zeta^2 \tag{3}$$

The probability P that an error vector of q degrees of freedom lies outside the q-dimensional ellipsoid specified by a particular value of ζ^2 is obtainable from tables of "Chi-square" distribution for q degrees of freedom, with $\zeta^2 = \chi^2$.** The probability that a given error ellipsoid contains the error vector is 1 - P.

---

* Note that $\begin{bmatrix} \epsilon_x^2 & \mu_{yx} & \mu_{zx} \\ \mu_{xy} & \epsilon_y^2 & \mu_{zy} \\ \mu_{xz} & \mu_{yz} & \epsilon_z^2 \end{bmatrix}^{-1}$ is the inverse of the 3×3 position covariance submatrix, which is not the same as the corresponding 3×3 submatrix of the 6×6 inverse covariance (information) matrix. Likewise for the 3×3 velocity covariance submatrix.

** T. W. Anderson, Introduction to Multivariate Statistical Analysis, John Wiley and Sons, 1958, p. 54.

In the three-dimensional error ellipsoids ($q = 3$), a choice of $\zeta = 1$ corresponds to an ellipsoid possessing a 20% probability that the error is contained within its bounds*.

Figure A-0 contains a curve, derived from a "Chi-Square" distribution table**, showing the probability that error is contained within the three-dimensional error ellipsoid, as a function of ζ. This means that scaling every dimension of an ($\zeta = 1$)-ellipsoid by, say, $\zeta = 2$, results in an ellipsoid possessing 73% probability of containing the error vector.

All the computations in this study are presented in terms of $\zeta = 1$, and Fig. A-0 is enclosed as a scaling aid.

Four quantities are chosen as measures of the "size" of the uncertainty, or error, associated with a trajectory estimate at a given epoch of estimation. They are defined in terms of the traces and determinants of the position and velocity covariance submatrices (t_p, d_p, t_v, d_v), and are interpreted both in terms of the geometry of the appropriate 3×3 error ellipsoids and of their significance as measures of estimation uncertainty:

---

* I. e., there is a 20% probability that the position error is contained within the position error ellipsoid, and there is a 20% probability that the velocity error lies within the velocity error ellipsoid, but no information is conveyed as to the probability of <u>both</u> conditions being satisfied. The missing information is associated with the position-velocity covariance terms of the 6×6 covariance matrix which are absent from equations (2) and (3).

** Paul G. Hoel, <u>Introduction to Mathematical Statistics</u>, 2nd Ed., John Wiley and Sons, 1954, Table III, p. 318.

Symbol of Error Measure	Definition in Terms of Covariance Matrix	Units of Measure	Interpretation in Terms of Error Ellipsoid of a Chosen "ξ"	Significance as Measure of Uncertainty
ϵ_p	$\sqrt{t_p/3}$	ft.	$\frac{1}{\xi} \times \left[\text{Rms}^{*} \text{ radius of the position error ellipsoid}\right]$	Rms* of the standard deviation of position errors over the 3 spatial components.
η_p	$d_p^{1/6}$	ft.	$\frac{1}{\xi} \times \left[\text{Radius of a sphere whose volume is equal to that of the position error ellipsoid}\right]$	Geometric mean of the standard deviation of position errors over the 3 spatial components.
ϵ_v	$\sqrt{t_v/3}$	ft. /sec.	$\frac{1}{\xi} \times \left[\text{Rms}^{*} \text{ radius of the velocity error ellipsoid}\right]$	Rms* of the standard deviation of velocity errors over the 3 spatial components.
η_v	$d_v^{1/6}$	ft./sec.	$\frac{1}{\xi} \times \left[\text{Radius of sphere whose volume is equal to that of the velocity error ellipsoid}\right]$	Geometric mean of the standard deviation of velocity errors over the 3 spatial components.

Note that $\epsilon_p \geq \eta_p$ and $\epsilon_v \geq \eta_v$. For this reason the ϵ's are the more conservative measures to use.

Furthermore, the velocity estimation errors are relatively less dependent on the particular epoch of estimation selected** and hence are usually a better measure of the overall quality of a trajectory estimate. For this reason the rms velocity error, ϵ_v, will be the one generally used measure in this report.

---

* "Root-mean-square".

** Over a small fraction of an orbit; not necessarily true for more extended translations along the nominal orbit.

The computations performed as part of this analysis were performed with the aid of a "general purpose" digital trajectory error analysis program for the IBM 7090, called PATE I*.

This program sees the true trajectory of a vehicle as the six-dimensional vector sum of a nominal Keplerian trajectory (in practice, usually equivalent to the estimated path), and a random position and velocity error vector, which is a random process with zero mean and a computable inverse covariance matrix.

In calculating the inverse covariance matrix of the six-dimensional error vector for a given epoch, a matrix of linearized partial derivatives of the non-linear equations of motion is used. This linearized procedure is valid if the error vector is small compared to the velocity and dimensions of the orbit, but decreases in validity if very large estimation errors are to be computed. It has been found, however, that the range of validity far exceeds the range of practical interest for the cases studied. (Deviations as large as 30,000 ft. and 200 ft./sec. have been found to introduce no observable discrepancy as a result of the linear approximation, in the near-earth case.)

The inverse covariance matrix is a function of the nominal trajectory and of the information contributions from each radar measurement and all other sources of trajectory knowledge, if any.

Measurements to Estimates

This analysis does not include consideration of problems of data assembly, transmission, and processing. In any practical situation, these are undoubtedly an important factor. This analysis assumes perfect communications with no information loss. This implies, of course, that any deviation from these conditions will result in poorer estimates than those indicated by the results obtained. This analysis probes the question, how

---

* "Program for the Analysis of Trajectory Estimation, No. 1," prepared by Charles W. Adams Associates, Inc., Bedford, Mass., under Lincoln Laboratory's joint service general research contract, in cooperation with Dr. Fred C. Schweppe of Lincoln Laboratory.

good an estimate is it possible to obtain with all available information? Some insight will be gained also regarding the question, of which information is more important and which is less important in trajectory estimation in a given situation? The latter considerations are of importance, not only in evaluating and specifying radar characteristics, but also in planning or evaluating the data transmission and processing aspects of a ground network as well.

The manner in which the total information - derived from radar measurements and a priori knowledge - is considered to be assembled and transformed into an estimate in the presently reported work is briefly as follows.

Each independent measurement or combination of measurements provides information about the trajectory, the "goodness" of which is describable by an information matrix. In terms of that time at which the radar takes the measurement (in one or several components of position or rate of movement), this information matrix is the information matrix of the measurement itself. For a radar making mutually independent measurements in range, azimuth angle, elevation angle, and range-rate, the information matrix of the measurements made at any one instant of time is as follows[*]:

$$\begin{matrix} 1/\sigma_R^2 & 0 & 0 & 0 & 0 & 0 \\ 0 & 1/\sigma_A^2 R^2 & 0 & 0 & 0 & 0 \\ 0 & 0 & 1/\sigma_A^2 R^2 & 0 & 0 & 0 \\ 0 & 0 & 0 & 1/\sigma_{\dot{R}}^2 & 0 & 0 \\ 0 & 0 & 0 & 0 & 0 & 0 \\ 0 & 0 & 0 & 0 & 0 & 0 \end{matrix}$$

---

* The angular variances have been multiplied here by the square of the range (best available estimate of the range), in order to convert them to position variance components.

It is only a matter of computation to transform this information matrix to conform with any other coordinate system desired.

Since some knowledge of the trajectory is always implicity assumed to be available (as otherwise no acquisition nor tracking of the vehicle would be possible), one can (at least approximately*) propagate the information of each successive measurement (as per its information matrix) to some chosen reference point in the orbit, where the contributions of each measurement (and of any additional sources of information, if any) are added together, by addition of information matrices**. In practical situations, a great variety of diverse schemes of processing tracking data are possible. The estimation errors, as computed herein, are merely reflections of the total information, which, in the absence of information losses, is conserved regardless of the particular data processing scheme used.

An exposition and discussion of the results of this investigation follows.

Results: The Computations

Graphs showing the computed estimation errors for the "basic radar," "basic radar times 10," and "basic radar times 1/10,"*** operating at 10 measurements per second, appear in Figures A-1 through A-12 in the Appendix. These graphs are in the form of ϵ_p, η_p, ϵ_v, or η_v, respectively, vs. σ_A. No a priori information has been introduced into the situations covered by Figures A-1 through A-12.

---

* The discrepancy introduced here is ordinarily expected to be of secondary significance, and is ignored in the present analysis.

** This additive property of the inverse covariance matrix is the reason why it is called the information matrix. If it is desired to consider losses of information (e.g., due to limitations of transmission facilities, or "editing" of the information data, or possibly other reasons), these considerations could be introduced as matrices to be added or subtracted from the information matrix.

*** See table on page 8 for the radar characteristics, and the section entitled, "Situations Considered: The Radar," (pp 6-8) for a discussion of their meaning, and of procedures for making the data applicable to other situations.

Figures A-13 through A-18 show the components of the estimation errors ("basic radar") in a vehicle-centered rectangular coordinate system*. In this coordinate system, the X-axis lies along the direction of motion, the Y-axis is normal to the trajectory and parallel to the orbital plane, and the Z-axis is normal to the orbital plane.

Figures A-19 and A-20 show the effect of <u>a priori</u> information on ϵ_p and ϵ_v, respectively. Representative situations with spherical <u>a priori</u> estimation error volumes are shown to illustrate the conclusions drawn (in subsequent paragraphs).

Figures A-21 and A-22 illustrate the effect on the trajectory estimation uncertainties of improving range-rate measurement accuracy of the radar, relative to its range measurement accuracy. Only velocity estimation errors are presented. These are expressed as a percentage of the estimation error in the absence of a range-rate measuring capability ($\sigma_R/\sigma_{\dot{R}} = 0$). The results given are for a nominal trajectory passing the radar at 4 degrees ECA. Note that the value of the ratio $\sigma_R/\sigma_{\dot{R}}$ that has been adopted for the bulk of the work in this analysis is 20 seconds, which is very near the "break" point in the curves of Figures A-21 and A-22.

<u>Results: Discussion</u>

Inspection of the ϵ_p and ϵ_v curves in Figures A-1 through A-10 suggests the relative lack of dependency of ϵ_p and ϵ_v on range and range-rate measurement accuracy, for the ranges of values considered. For a near-earth orbital vehicle tracked by a single radar site having any reasonable range measuring capability, <u>the angle measuring capability is the determining factor in the radar's trajectory estimating capability</u>**. This statement is not true for a radar lacking both range and range-rate capability, and it may not be true for a radar having only range-rate capability in addition to the angle-capability, but for radars falling within the range of values:

---

* They contain no information about the amount of correlation between the various components, however.

** Measured in terms of ϵ_p and ϵ_v.

$$0 < \sigma_R/\sigma_A < 1000 \text{ ft. /milliradian}$$

$$0 < \sigma_R/\sigma_{\dot{R}} < 30 \text{ seconds} ,$$

the estimation errors are only feebly dependent on σ_R and $\sigma_{\dot{R}}$. Under these conditions, the relationship is effectively:

$$\epsilon_p = K_1 \sigma_A$$

$$\epsilon_v = K_2 \sigma_A .$$

(The relationships of η_p and η_v to σ_A are somewhat different, but they are of lesser interest and are not considered here.)

To explain these phenomena, consider the critical region in the $\sigma_R/\sigma_{\dot{R}}$ ratio, i.e., $\sigma_R/\sigma_{\dot{R}} \approx 10$ to 100 seconds (See figure A-21). <u>If $\sigma_{\dot{R}}$ (in ft. /sec.) is larger than about $\sigma_R/30$ (with σ_R in ft.), the errors of estimation are only insignificantly smaller than if no range-rate capability existed at all ($\sigma_{\dot{R}} = \infty$).</u> (See figures A-21 and A-22). The conclusion that can be drawn is that for all the situations considered, where $\sigma_R/\sigma_{\dot{R}}$ was selected at 20 seconds, the results are equivalent, virtually without alteration, for radars measuring range, azimuth and elevation only. The effects of the angle measuring capability will be considered in the context of a range-and-angles-only radar.

The tracked segment of the orbit can be considered to be effectively a segment of a straight line, and hence the tracking beam will at all times lie in the plane defined by the trajectory and the site location. That component of each measurement error ellipsoid which is normal to this plane will consistently be independent of σ_R. It is determined solely by the azimuth and elevation measurement errors. Consequently, whenever RANGE $\times\ \sigma_A$ (in radians) is substantially larger than σ_R, this component of error will predominate also in the final estimation error ellipsoid. Since the effective range* for the situations considered is on the order of 1 to 3 million feet, we expect the rms estimation errors to be effectively a function of angle accuracy only whenever $\sigma_R/\sigma_A \ll$ EFFECTIVE RANGE $\approx 10^6$, or $\ll$ (EFFECTIVE RANGE/1000), if we express σ_A in milliradians. This checks with the observation. Also, the above bound effectively contains most situations of practical interest.

Figures A-23 and A-24 show the essentially limiting situations with "perfect" (i.e., $\sigma_R/\sigma_A \approx 0$) range accuracy (and thus, of course, effectively devoid of significant range-rate information, as per above discussions regarding $\sigma_R/\sigma_{\dot{R}} < 30$). These curves were drawn as the lower asymptotes to the ϵ_p and ϵ_v curves in Figures A-1 through A-10. The significance lies in the fact that they represent the lower limits on the size of rms estimation errors that can be obtained by a single radar site. They show that this lower limit is dependent on σ_A only, and no improvement in the range or range-rate capability can lower the size of the error past these limits. If it is not possible to improve σ_A, outside sources of information have to be enlisted in order to further improve the estimates. In order to be effective, they must provide information specifically about those components which the radar site is least capable of measuring. i.e., they must provide <u>improved</u> measurements of the vehicles position <u>in the component normal</u> to the plane containing its path and the radar site.

One means to obtain this needed additional information is to have an additional site located so that the plane it defines with the trajectory is as nearly perpendicular as possible to that of the first site**.

---

* Computable over the tracking interval by the expression $\left(\frac{1}{M}\sum_{i=1}^{M}\frac{1}{R_i^2}\right)^{-1/2}$ where M = number of measurements, and R_i is the range at the time of the i-th measurement.

** Both sites should be located near to one another, (not more than about 1/8 of an orbit apart). The combined capability of two (or several) sites further removed from one another can be expected to involve other considerations.

Another means is a priori information about the trajectory from other sources. As was mentioned in the section entitled, "Measurements to Estimates," some a priori knowledge is always implicitly assumed even in those situations labeled "No a priori information" because it is essential in order for tracking to take place and for the formation of an estimate to be started. However, in order for a priori information to quantitatively influence the quality of a trajectory estimate provided by a radar site, it is required to be comparable or better than the accumulated information provided by the radar, in at least one of the components measured. In other words, the six-dimensional error ellipsoid of the a priori estimate (propagated to the epoch of estimation of the trajectory by the radar, or vice versa) must either intersect or be contained within the error ellipsoid of the estimate that would be provided by the radar alone, in order to make a significant contribution to the trajectory estimate.

Some computations with a priori information were performed in this phase of the study, but the a priori estimation error ellipsoids were chosen spherical in both position and velocity. Representative cases are shown in Figures A-19 and A-20.

In situations where the a priori estimation errors are equal to the radar-only estimation errors, the combined estimation error is expected to be about 70% of the a priori error. The reason is that basically a

$$\frac{1}{\sigma_1^2} + \frac{1}{\sigma_2^2}$$

type of information addition takes place. Actually, as was pointed out, it is two six-by-six information (inverse covariance) matrices that are added together, but the principle is analogous. This explains also why a priori information that is poorer than the information provided by the tracking data will fail to substantially influence the size of the final estimation errors.

Subject Areas for Further Study

An analytical study such as the one undertaken involves effort in any or all of the following three basic categories:

1. Actual or practical situations
2. Theory and hypothetical situations
3. Methods and tools of analysis.

A theoretically oriented study of judiciously chosen situations, making use of existing and available methods and tools, is more likely to produce meaningful and usable results than emphasis on the evaluation of situations of immediate practical concern. Future extensions of the present analysis will encompass at least some of the following topics:

a. More work in the study of single-site radar parameters, particularly the interplay between position-measurement and rate-of-motion-measurement information.

b. Two-site situations, where both sites are located in the same general position of the orbit.

c. Longer-distance propagation of estimation errors, and orbits which involve sites significantly removed from one another.

d. Consideration of bias errors in measurements.

e. Extensions to other than near-earth, near-circular trajectories.

JŠ:r

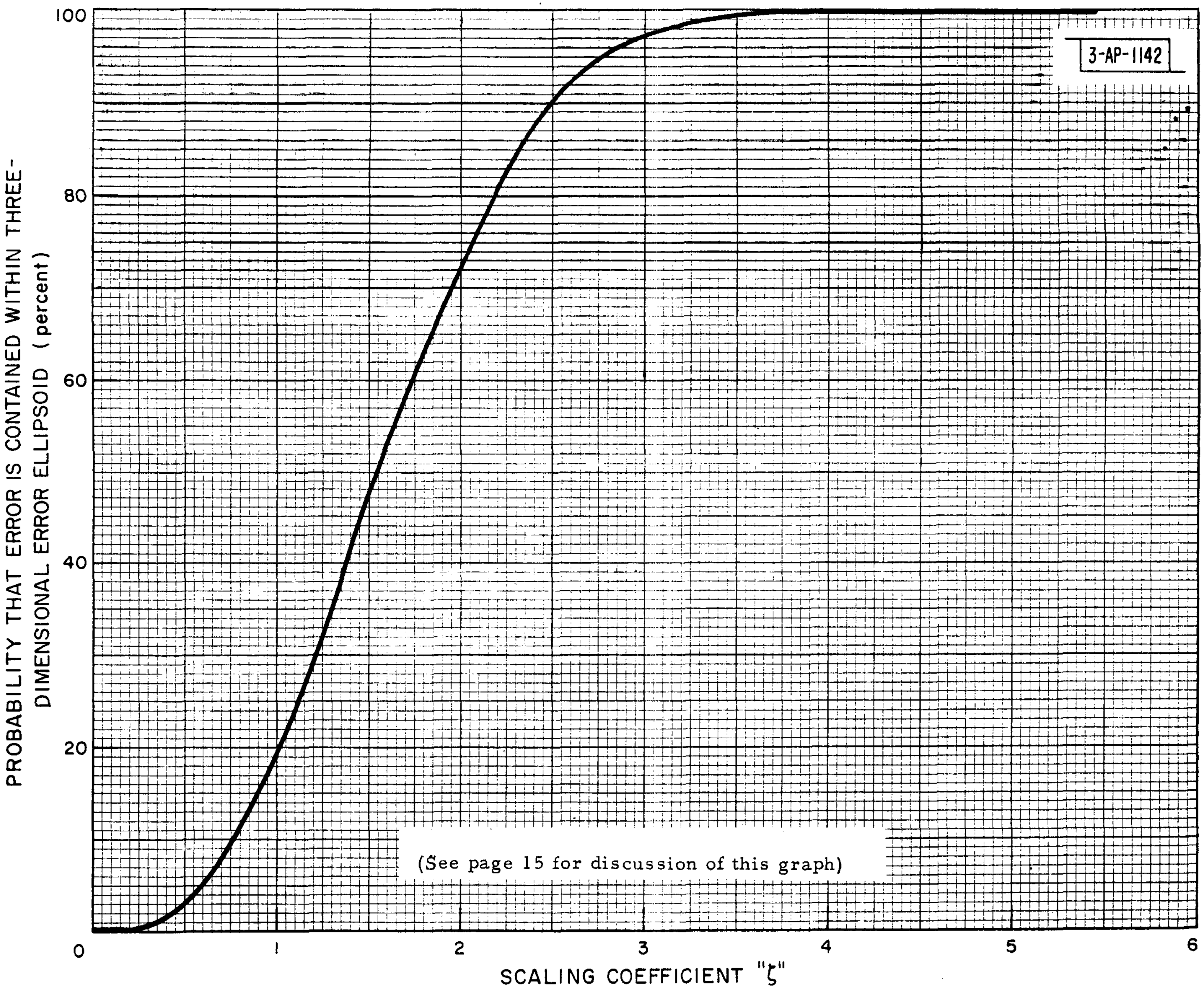

100
80
60
40
20
0
1
2
3
4
5
6
PROBABILITY THAT ERROR IS CONTAINED WITHIN THREE-DIMENSIONAL ERROR ELLIPSOID (percent)
SCALING COEFFICIENT "ζ"
3-AP-1142
(See page 15 for discussion of this graph)

Figure A-0

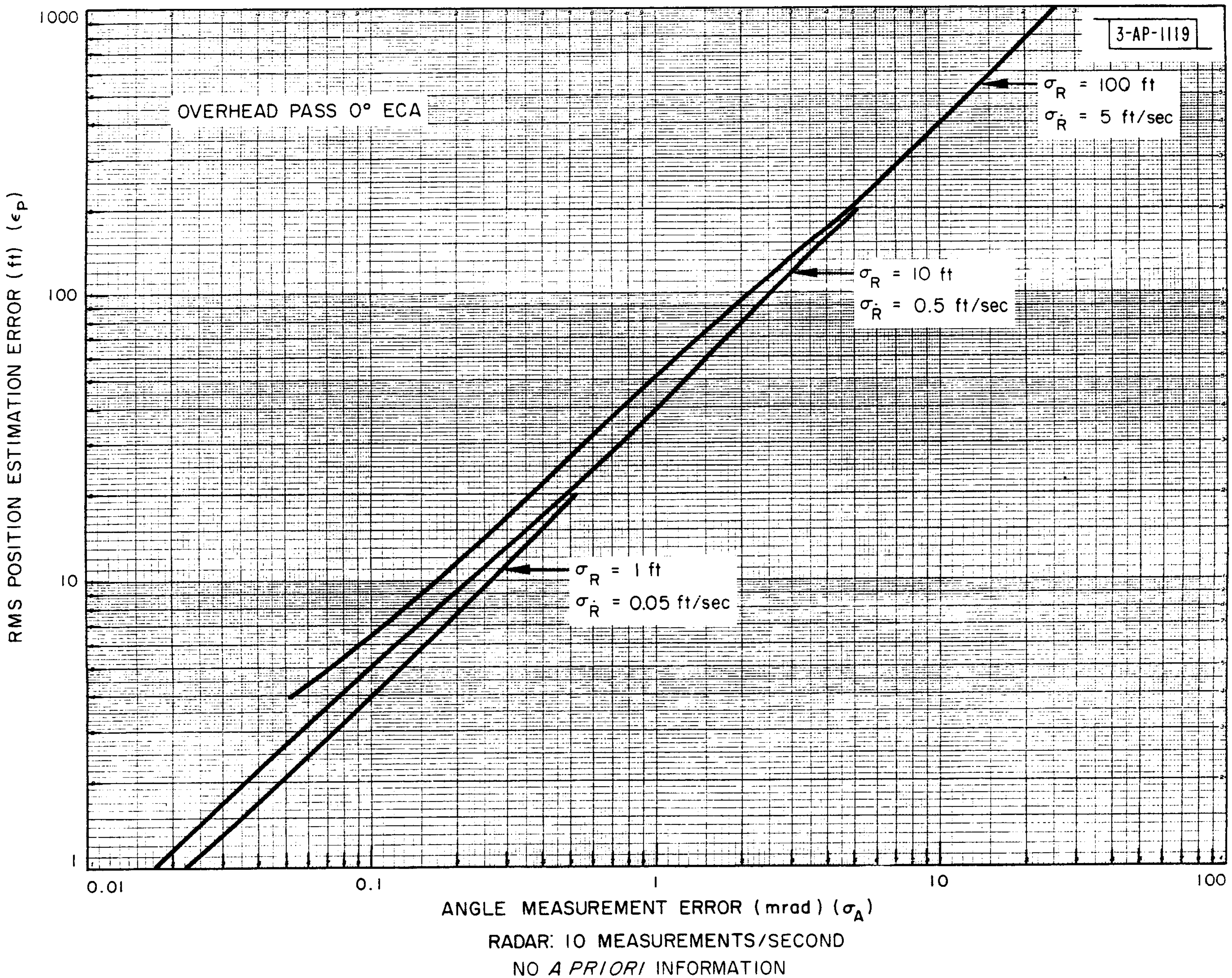
3-AP-1119
OVERHEAD PASS 0° ECA
σ_R = 100 ft
$\sigma_{\dot{R}}$ = 5 ft/sec
σ_R = 10 ft
$\sigma_{\dot{R}}$ = 0.5 ft/sec
σ_R = 1 ft
$\sigma_{\dot{R}}$ = 0.05 ft/sec
RMS POSITION ESTIMATION ERROR (ft) (ϵ_p)
1000
100
10
1
0.01
0.1
1
10
100
ANGLE MEASUREMENT ERROR (mrad) (σ_A)
RADAR: 10 MEASUREMENTS/SECOND
NO *A PRIORI* INFORMATION

Figure A-1

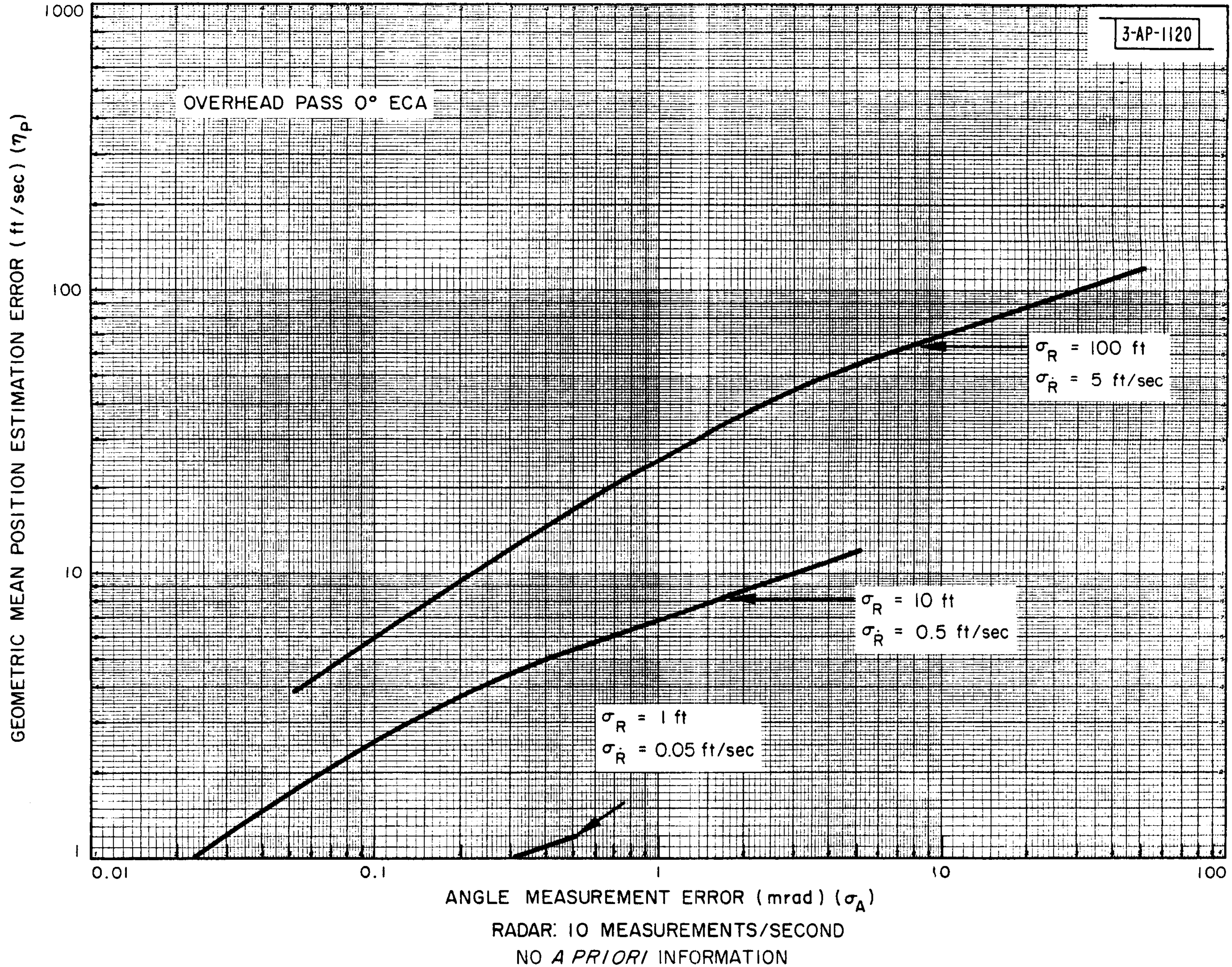

3-AP-1120
OVERHEAD PASS 0° ECA
GEOMETRIC MEAN POSITION ESTIMATION ERROR (ft / sec) (η_p)
1000
100
10
1
0.01
0.1
1
10
100
σ_R = 100 ft
$\sigma_{\dot{R}}$ = 5 ft/sec
σ_R = 10 ft
$\sigma_{\dot{R}}$ = 0.5 ft/sec
σ_R = 1 ft
$\sigma_{\dot{R}}$ = 0.05 ft/sec
ANGLE MEASUREMENT ERROR (mrad) (σ_A)
RADAR: 10 MEASUREMENTS/SECOND
NO *A PRIORI* INFORMATION

Figure A-2

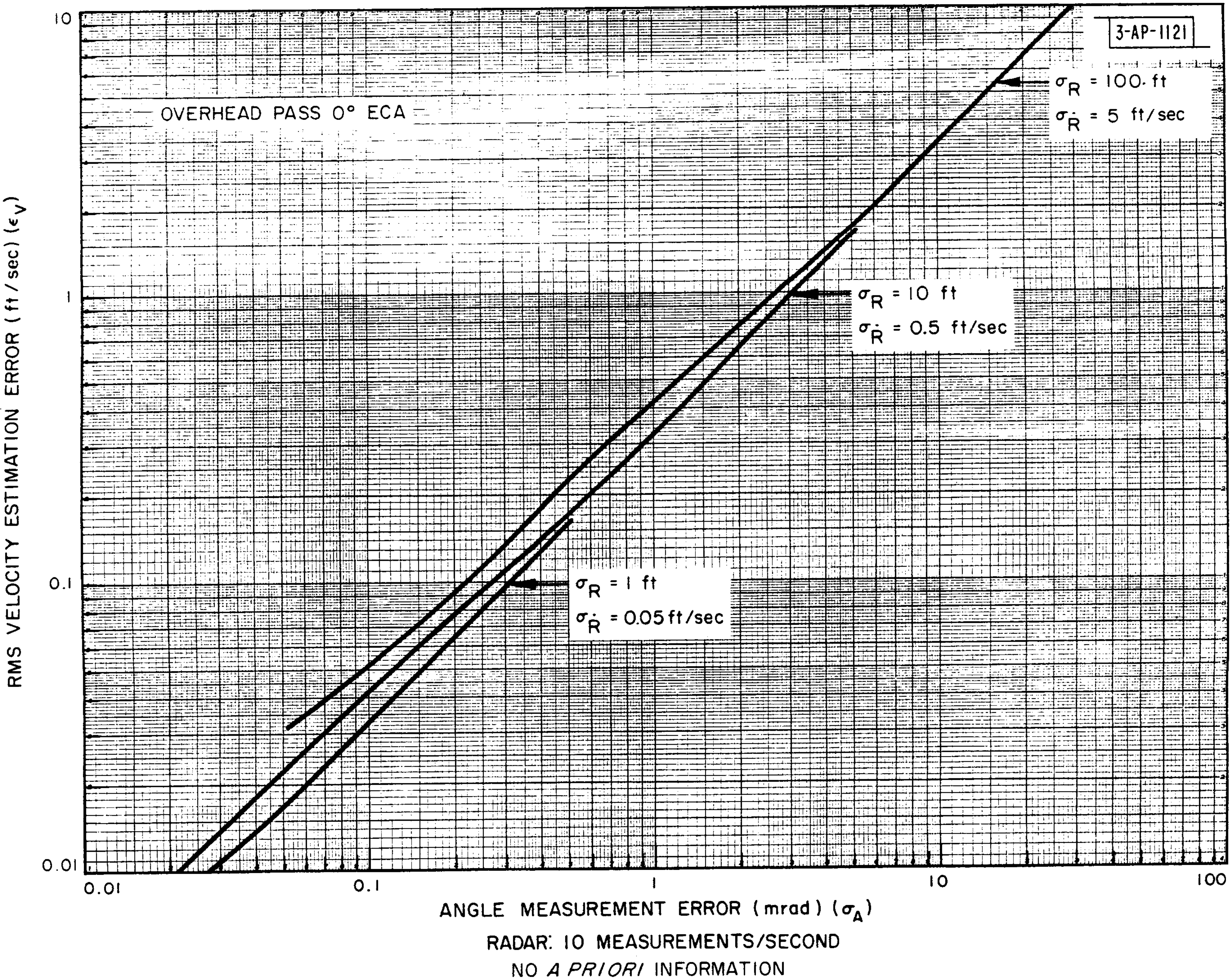
3-AP-1121
OVERHEAD PASS 0° ECA
σ_R = 100 ft
$\sigma_{\dot{R}}$ = 5 ft/sec
σ_R = 10 ft
$\sigma_{\dot{R}}$ = 0.5 ft/sec
σ_R = 1 ft
$\sigma_{\dot{R}}$ = 0.05 ft/sec
RMS VELOCITY ESTIMATION ERROR (ft/sec) (ϵ_V)
10
1
0.1
0.01
0.01
0.1
1
10
100
ANGLE MEASUREMENT ERROR (mrad) (σ_A)
RADAR: 10 MEASUREMENTS/SECOND
NO *A PRIORI* INFORMATION

Figure A-3

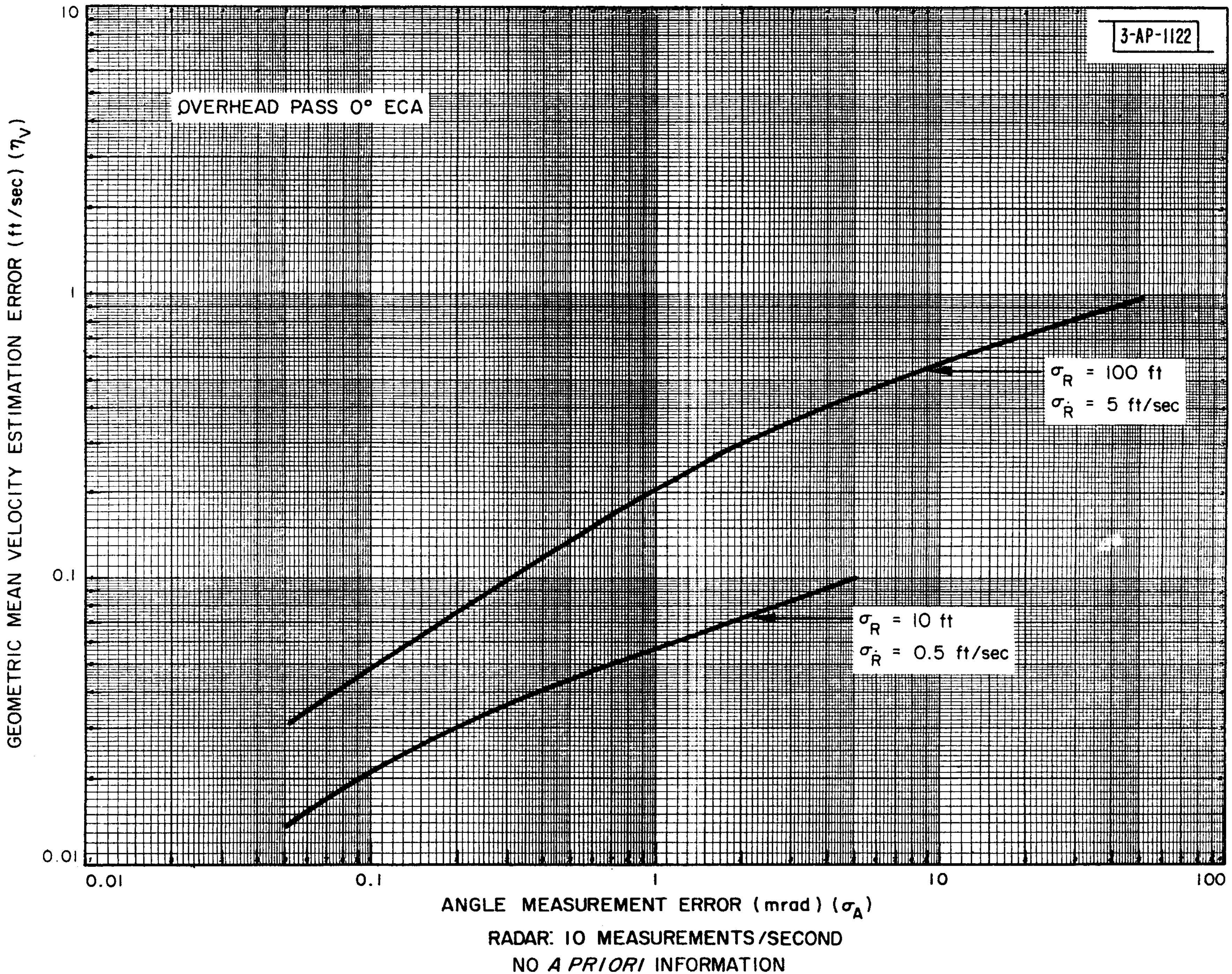
3-AP-1122
OVERHEAD PASS 0° ECA
GEOMETRIC MEAN VELOCITY ESTIMATION ERROR (ft/sec) (η_V)
10
1
0.1
0.01
σ_R = 100 ft
$\sigma_{\dot{R}}$ = 5 ft/sec
σ_R = 10 ft
$\sigma_{\dot{R}}$ = 0.5 ft/sec
0.01
0.1
1
10
100
ANGLE MEASUREMENT ERROR (mrad) (σ_A)
RADAR: 10 MEASUREMENTS/SECOND
NO *A PRIORI* INFORMATION

Figure A-4

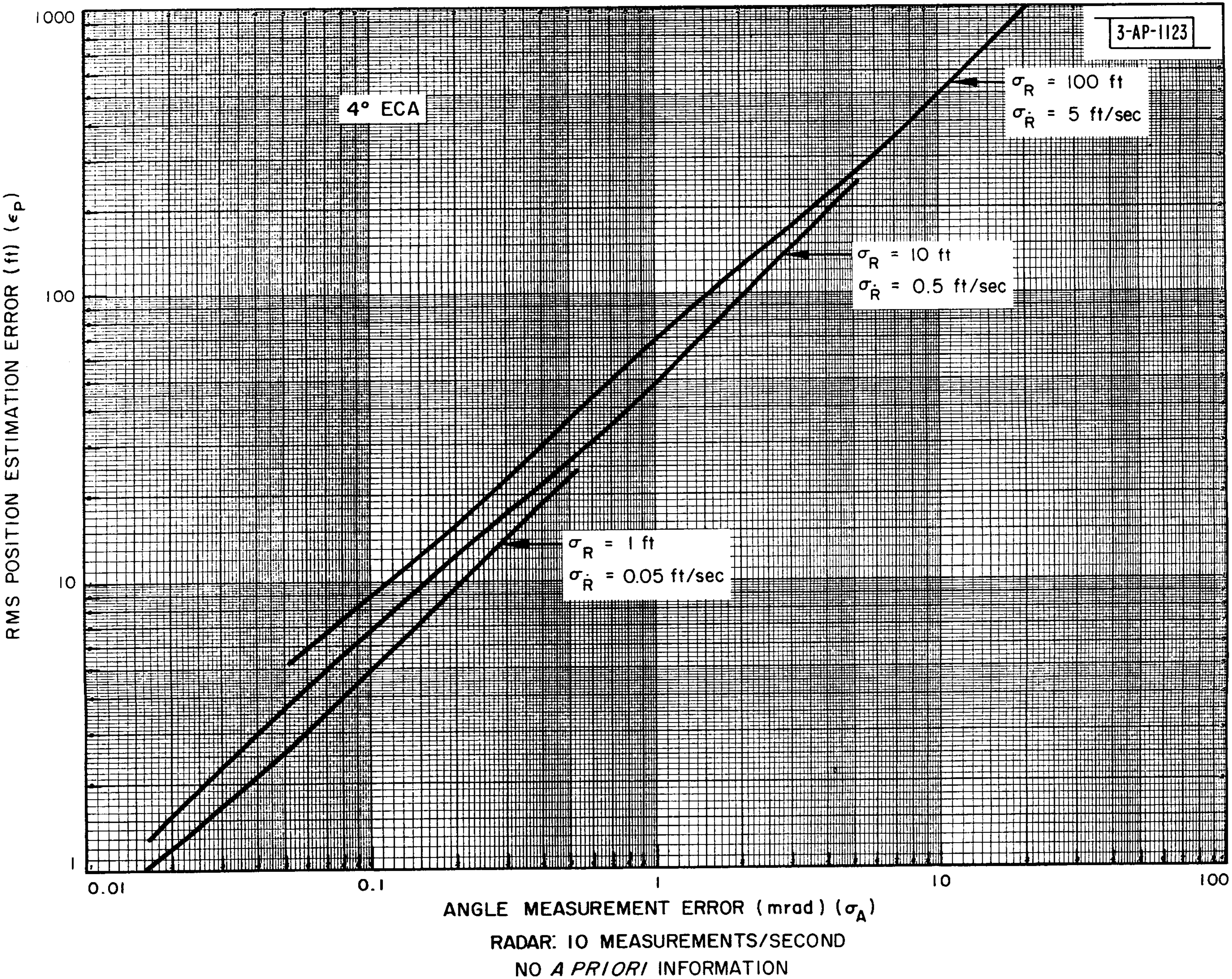

3-AP-1123
4° ECA
σ_R = 100 ft
$\sigma_{\dot{R}}$ = 5 ft/sec
σ_R = 10 ft
$\sigma_{\dot{R}}$ = 0.5 ft/sec
σ_R = 1 ft
$\sigma_{\dot{R}}$ = 0.05 ft/sec
RMS POSITION ESTIMATION ERROR (ft) (ϵ_p)
1000
100
10
1
0.01
0.1
1
10
100
ANGLE MEASUREMENT ERROR (mrad) (σ_A)
RADAR: 10 MEASUREMENTS/SECOND
NO *A PRIORI* INFORMATION

Figure A-5

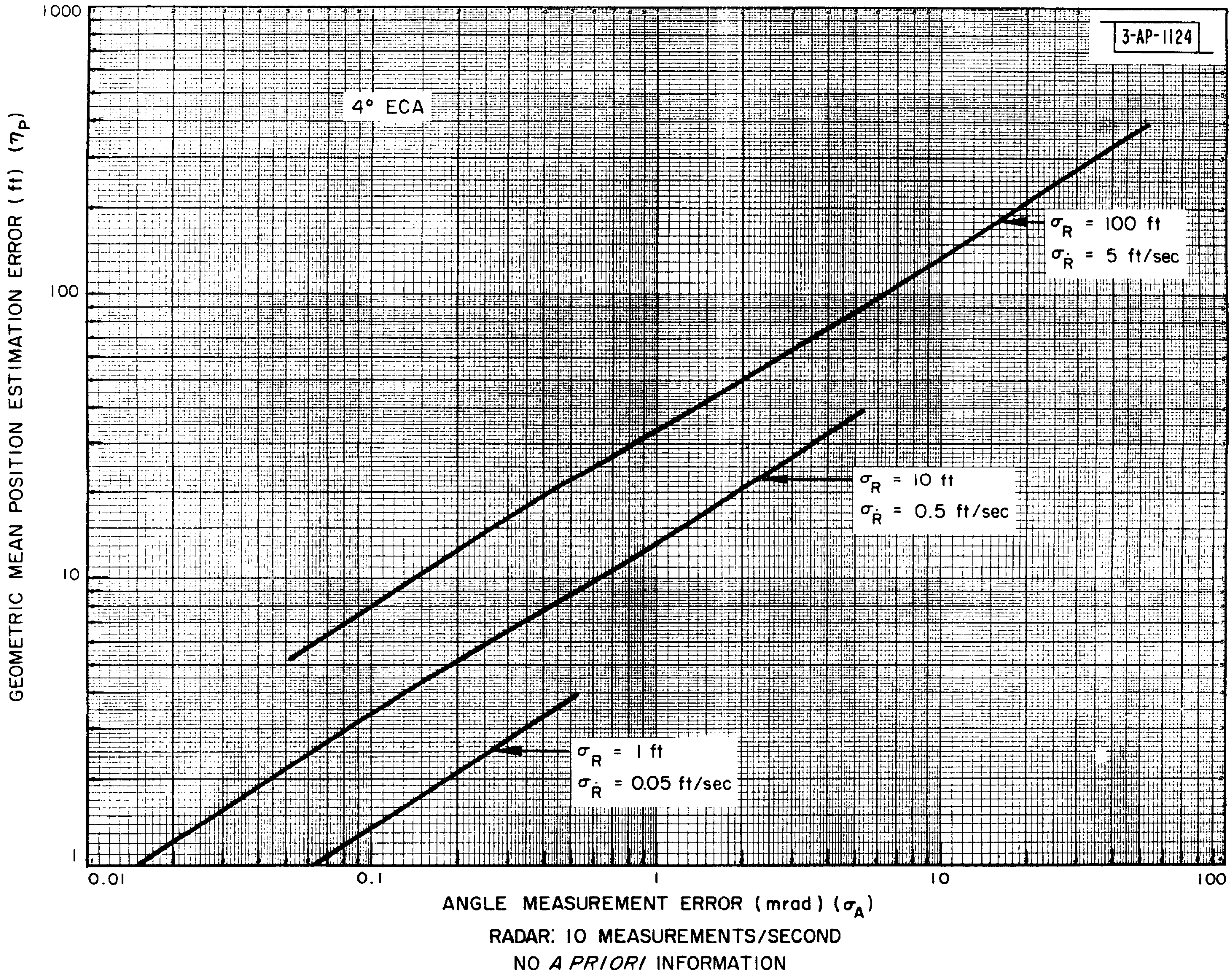
3-AP-1124
4° ECA
σ_R = 100 ft
$\sigma_{\dot{R}}$ = 5 ft/sec
σ_R = 10 ft
$\sigma_{\dot{R}}$ = 0.5 ft/sec
σ_R = 1 ft
$\sigma_{\dot{R}}$ = 0.05 ft/sec
GEOMETRIC MEAN POSITION ESTIMATION ERROR (ft) (η_p)
1000
100
10
1
0.01
0.1
1
10
100
ANGLE MEASUREMENT ERROR (mrad) (σ_A)
RADAR: 10 MEASUREMENTS/SECOND
NO *A PRIORI* INFORMATION

Figure A-6

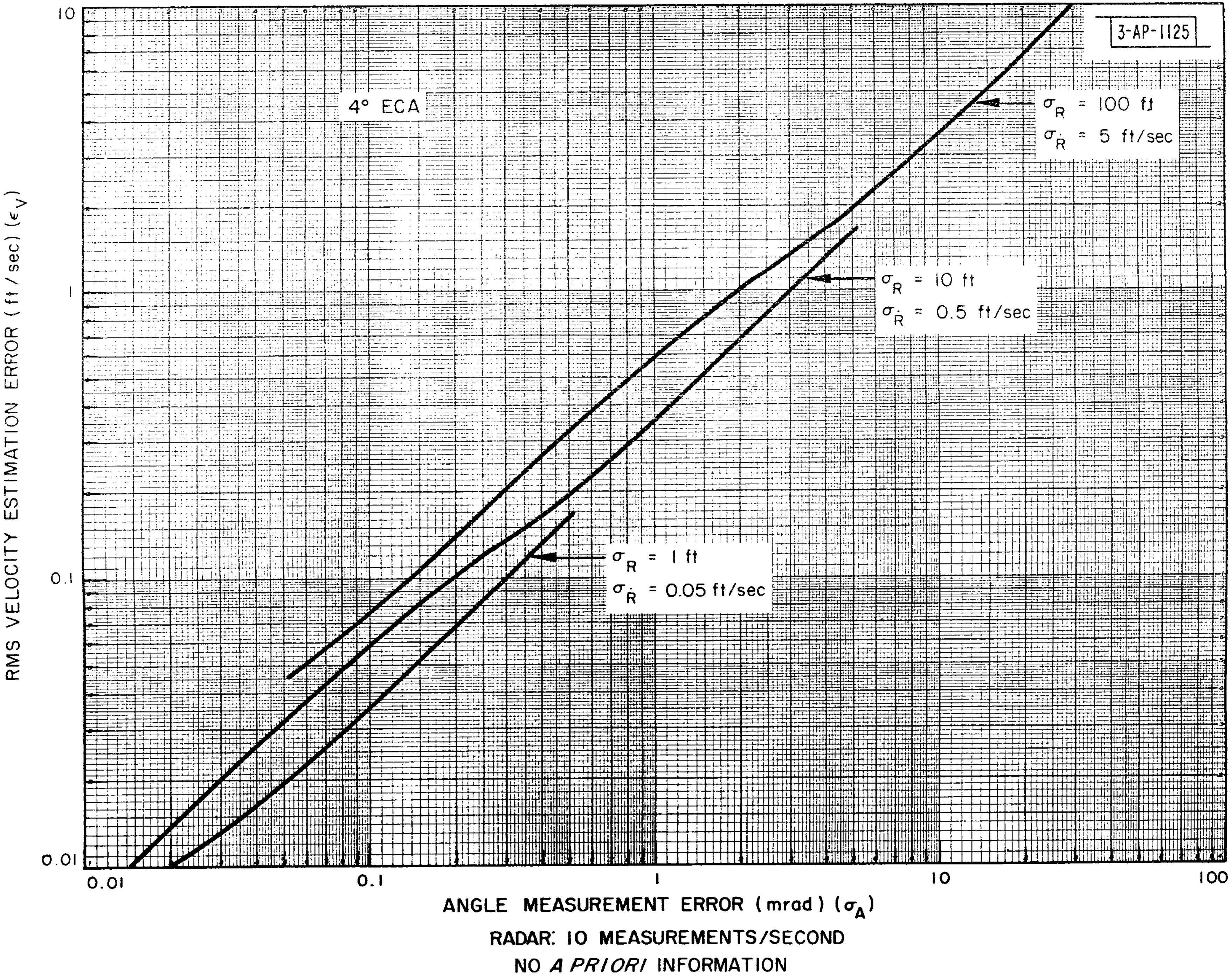
3-AP-1125
4° ECA
σ_R = 100 ft
$\sigma_{\dot{R}}$ = 5 ft/sec
σ_R = 10 ft
$\sigma_{\dot{R}}$ = 0.5 ft/sec
σ_R = 1 ft
$\sigma_{\dot{R}}$ = 0.05 ft/sec
RMS VELOCITY ESTIMATION ERROR (ft / sec) (ϵ_V)
10
1
0.1
0.01
0.01
0.1
1
10
100
ANGLE MEASUREMENT ERROR (mrad) (σ_A)
RADAR: 10 MEASUREMENTS/SECOND
NO *A PRIORI* INFORMATION

Figure A-7

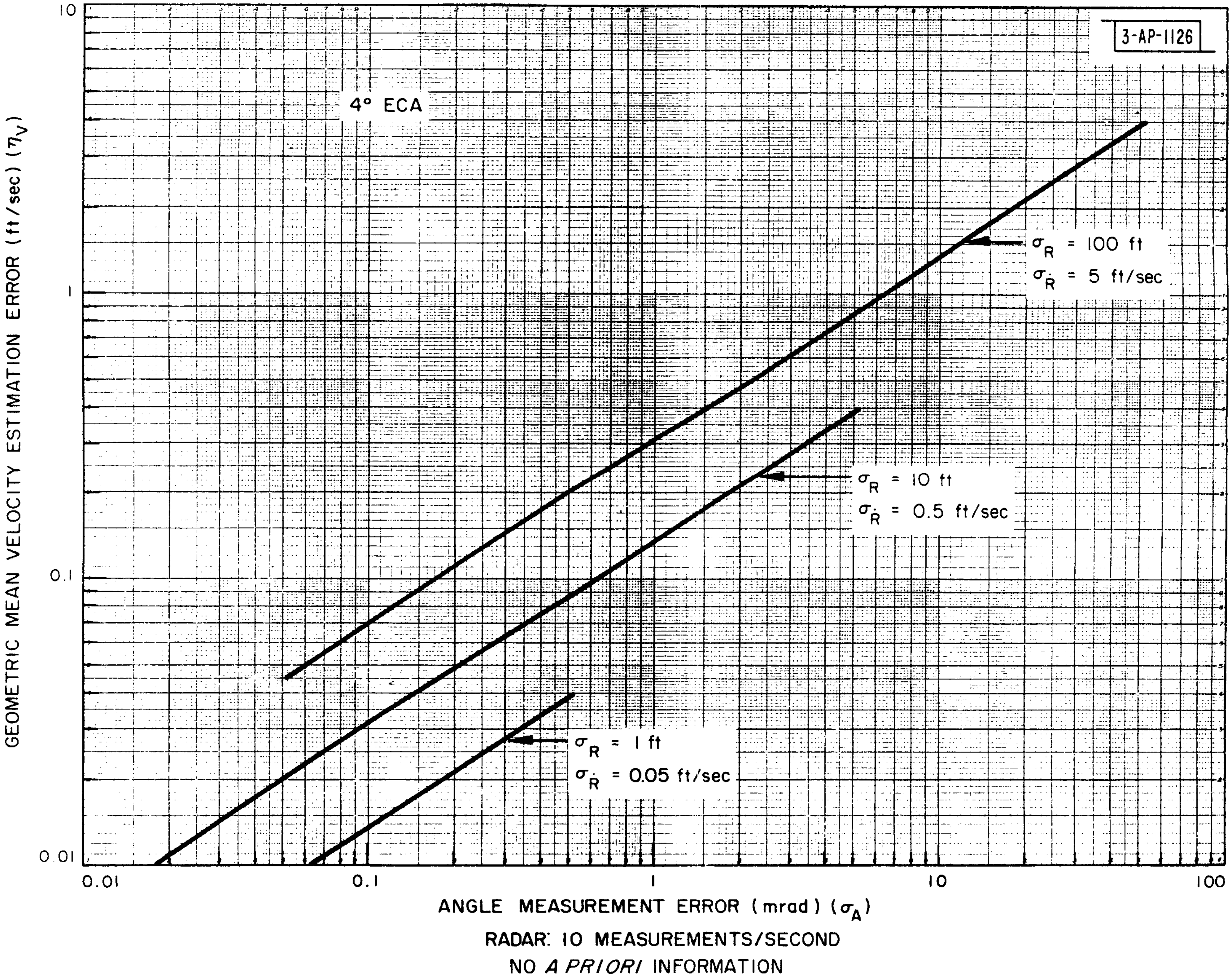

3-AP-1126
4° ECA
σ_R = 100 ft
$\sigma_{\dot{R}}$ = 5 ft/sec
σ_R = 10 ft
$\sigma_{\dot{R}}$ = 0.5 ft/sec
σ_R = 1 ft
$\sigma_{\dot{R}}$ = 0.05 ft/sec
GEOMETRIC MEAN VELOCITY ESTIMATION ERROR (ft/sec) (η_V)
10
1
0.1
0.01
0.01
0.1
1
10
100
ANGLE MEASUREMENT ERROR (mrad) (σ_A)
RADAR: 10 MEASUREMENTS/SECOND
NO *A PRIORI* INFORMATION

Figure A-8

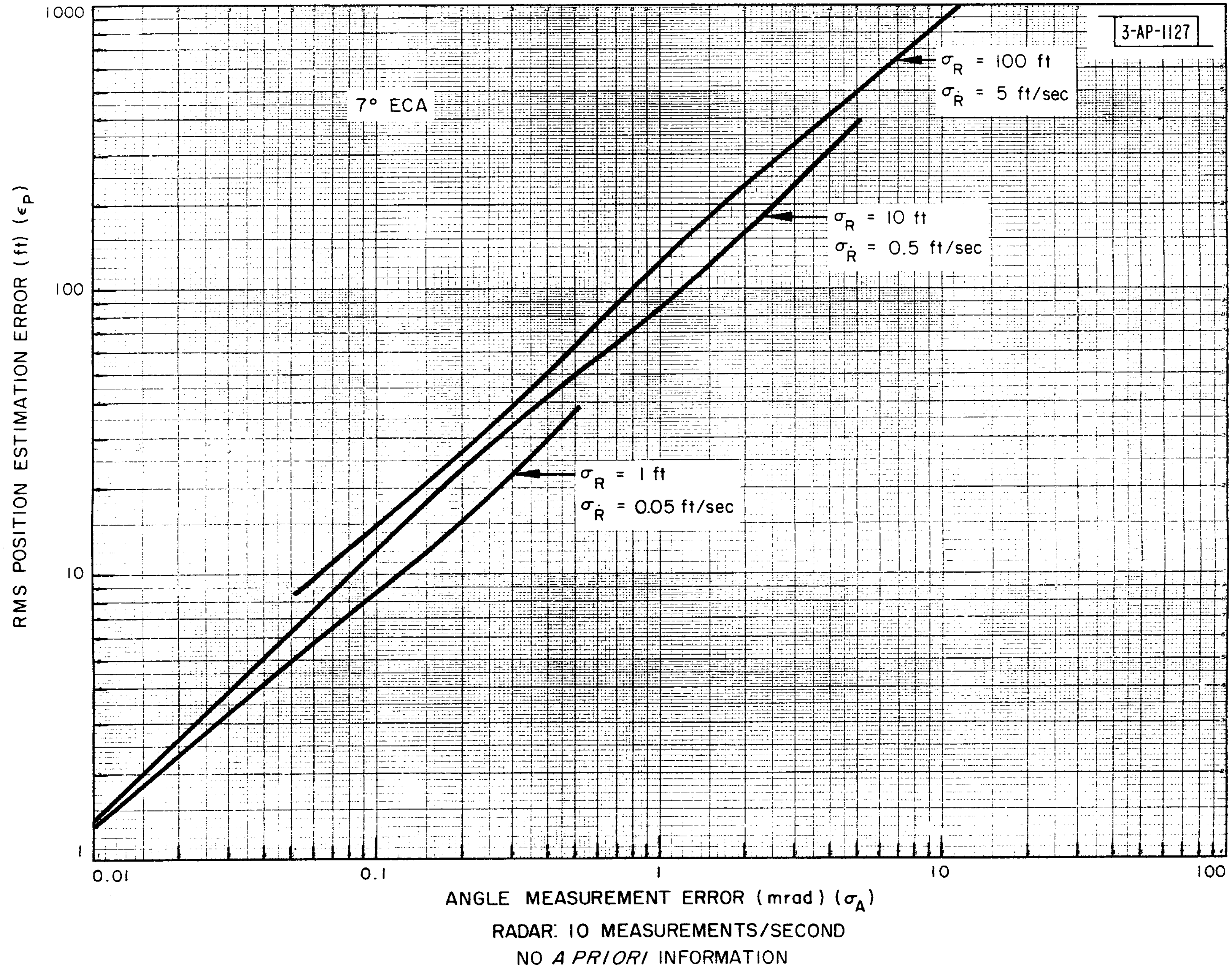
3-AP-1127
7° ECA
σ_R = 100 ft
$\sigma_{\dot{R}}$ = 5 ft/sec
σ_R = 10 ft
$\sigma_{\dot{R}}$ = 0.5 ft/sec
σ_R = 1 ft
$\sigma_{\dot{R}}$ = 0.05 ft/sec
RMS POSITION ESTIMATION ERROR (ft) (ϵ_p)
1000
100
10
1
0.01
0.1
1
10
100
ANGLE MEASUREMENT ERROR (mrad) (σ_A)
RADAR: 10 MEASUREMENTS/SECOND
NO *A PRIORI* INFORMATION

Figure A-9

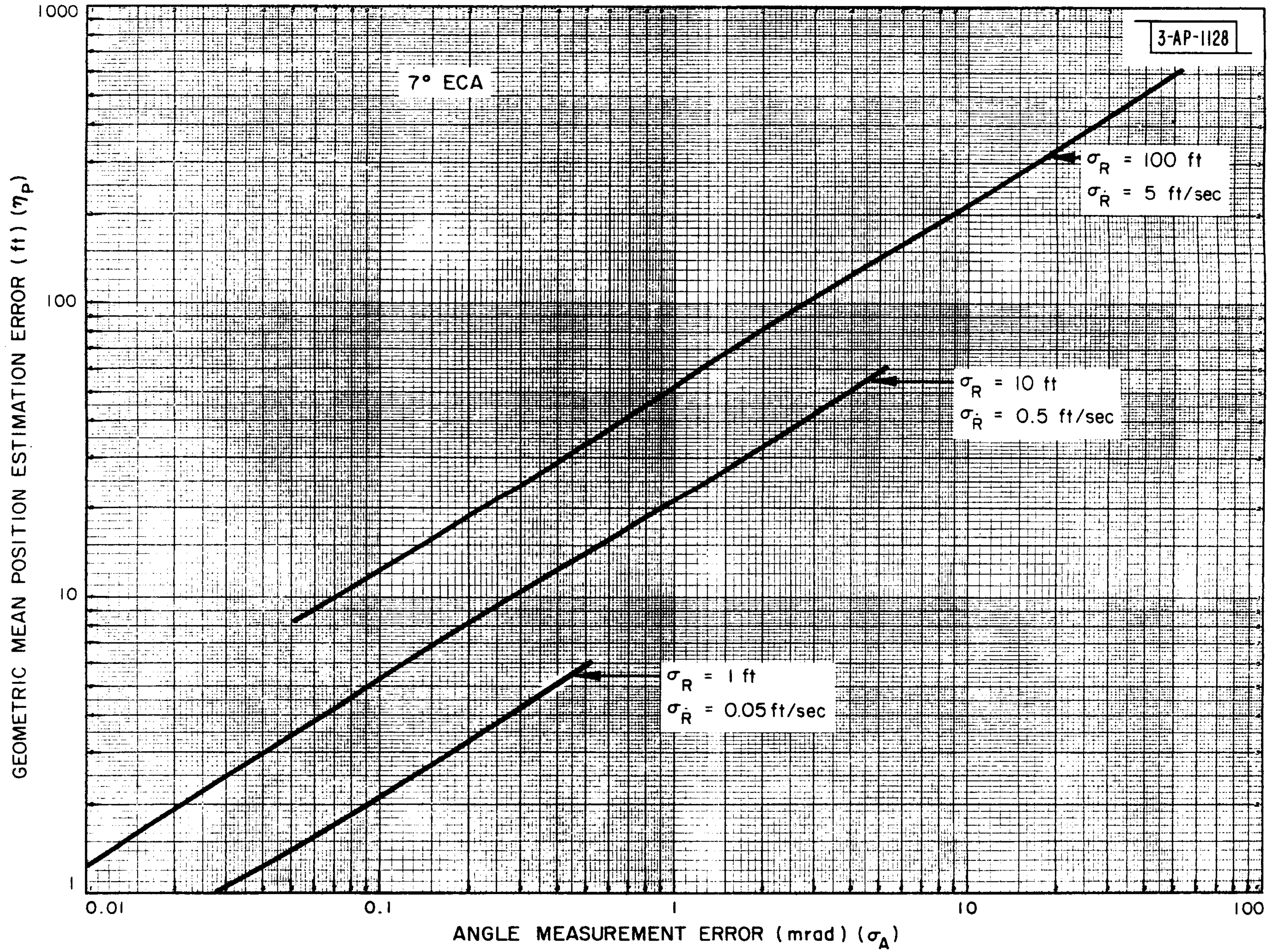

Figure A-10 RADAR: 10 MEASUREMENTS/SECOND
NO *A PRIORI* INFORMATION

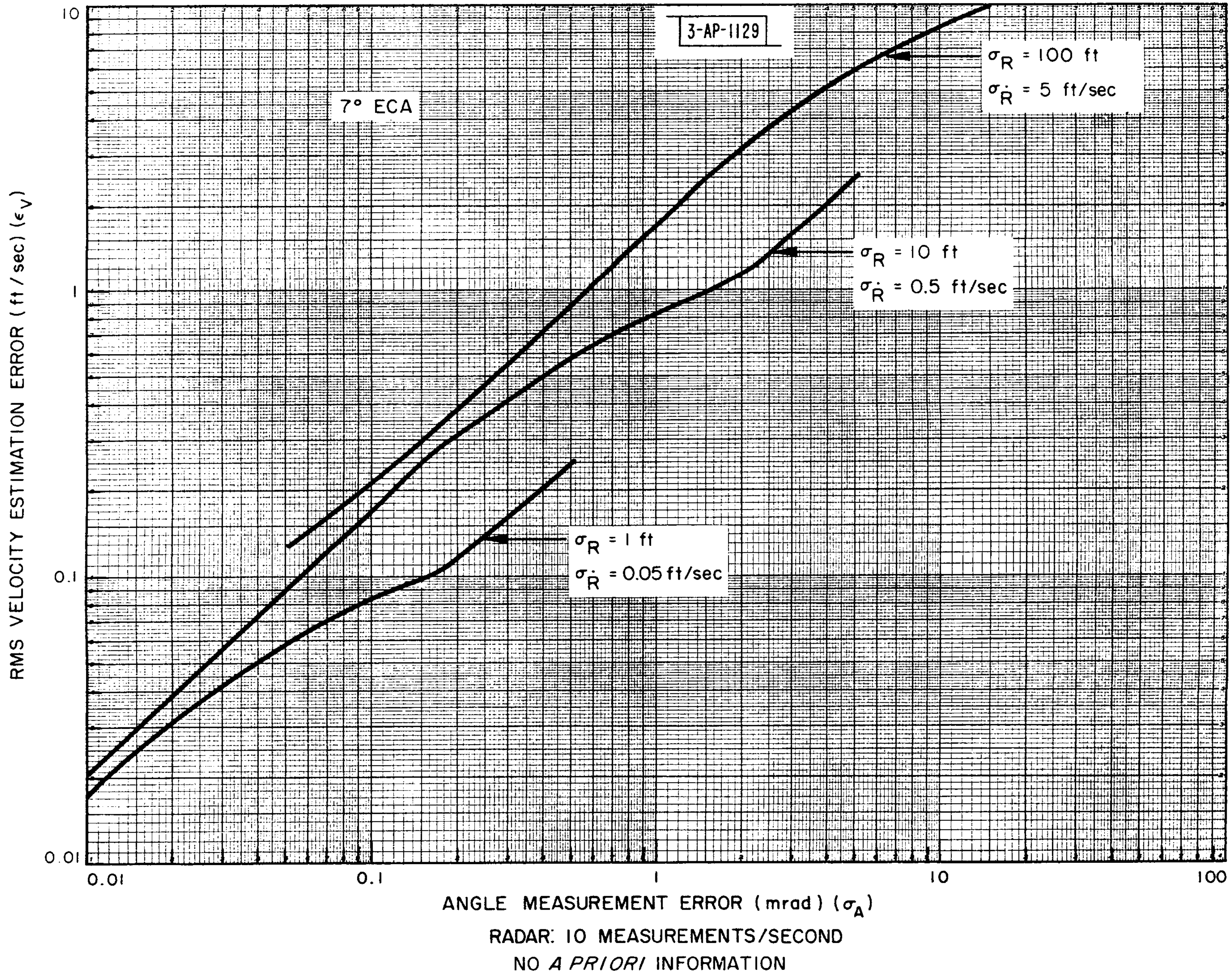
3-AP-1129
7° ECA
σ_R = 100 ft
$\sigma_{\dot{R}}$ = 5 ft/sec
σ_R = 10 ft
$\sigma_{\dot{R}}$ = 0.5 ft/sec
σ_R = 1 ft
$\sigma_{\dot{R}}$ = 0.05 ft/sec
RMS VELOCITY ESTIMATION ERROR (ft/sec) (ϵ_V)
10
1
0.1
0.01
0.01
0.1
1
10
100
ANGLE MEASUREMENT ERROR (mrad) (σ_A)
RADAR: 10 MEASUREMENTS/SECOND
NO *A PRIORI* INFORMATION

Figure A-11

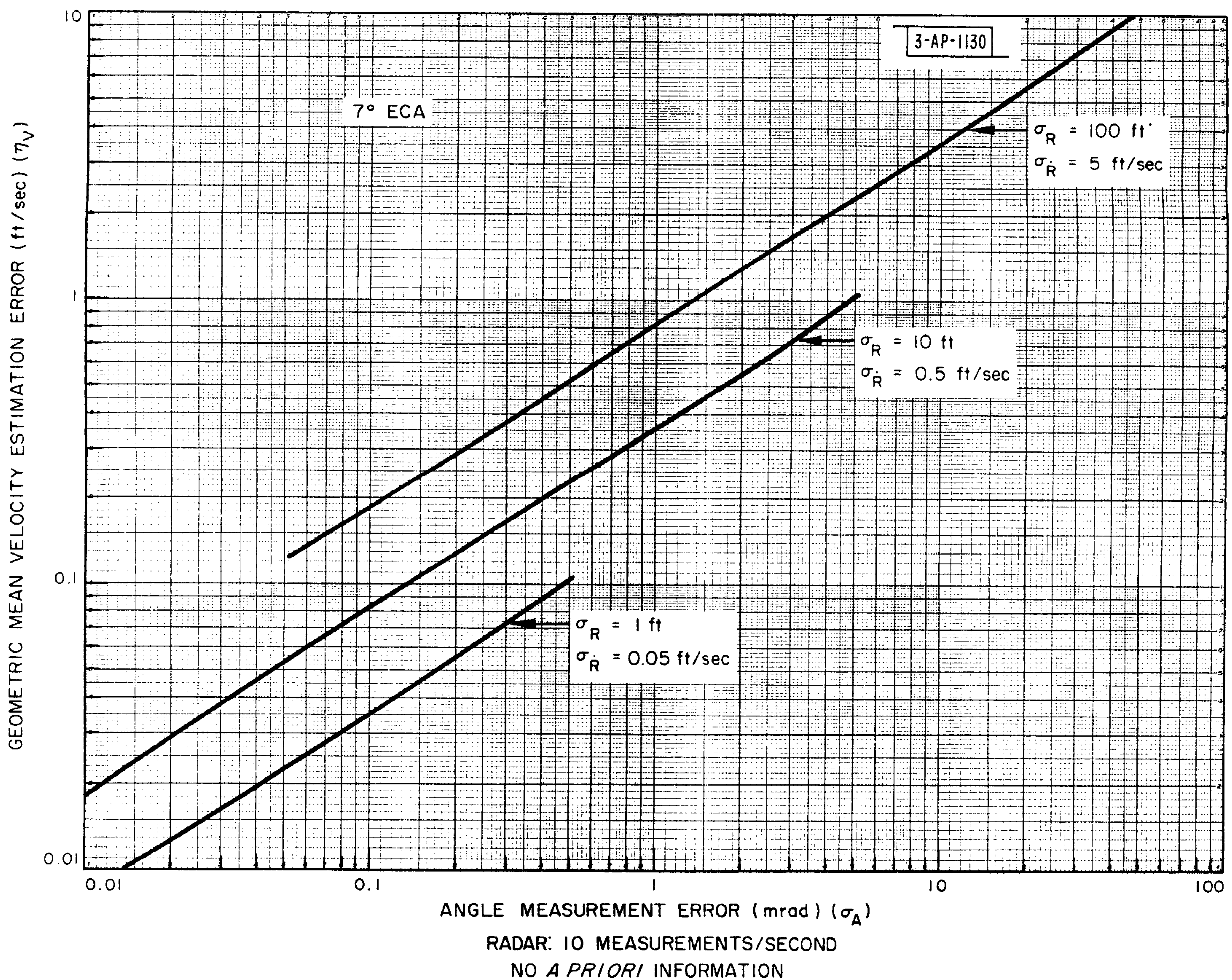
3-AP-1130
7° ECA
σ_R = 100 ft
$\sigma_{\dot{R}}$ = 5 ft/sec
σ_R = 10 ft
$\sigma_{\dot{R}}$ = 0.5 ft/sec
σ_R = 1 ft
$\sigma_{\dot{R}}$ = 0.05 ft/sec
GEOMETRIC MEAN VELOCITY ESTIMATION ERROR (ft/sec) (η_V)
10
1
0.1
0.01
0.01
0.1
1
10
100
ANGLE MEASUREMENT ERROR (mrad) (σ_A)
RADAR: 10 MEASUREMENTS/SECOND
NO *A PRIORI* INFORMATION

Figure A-12

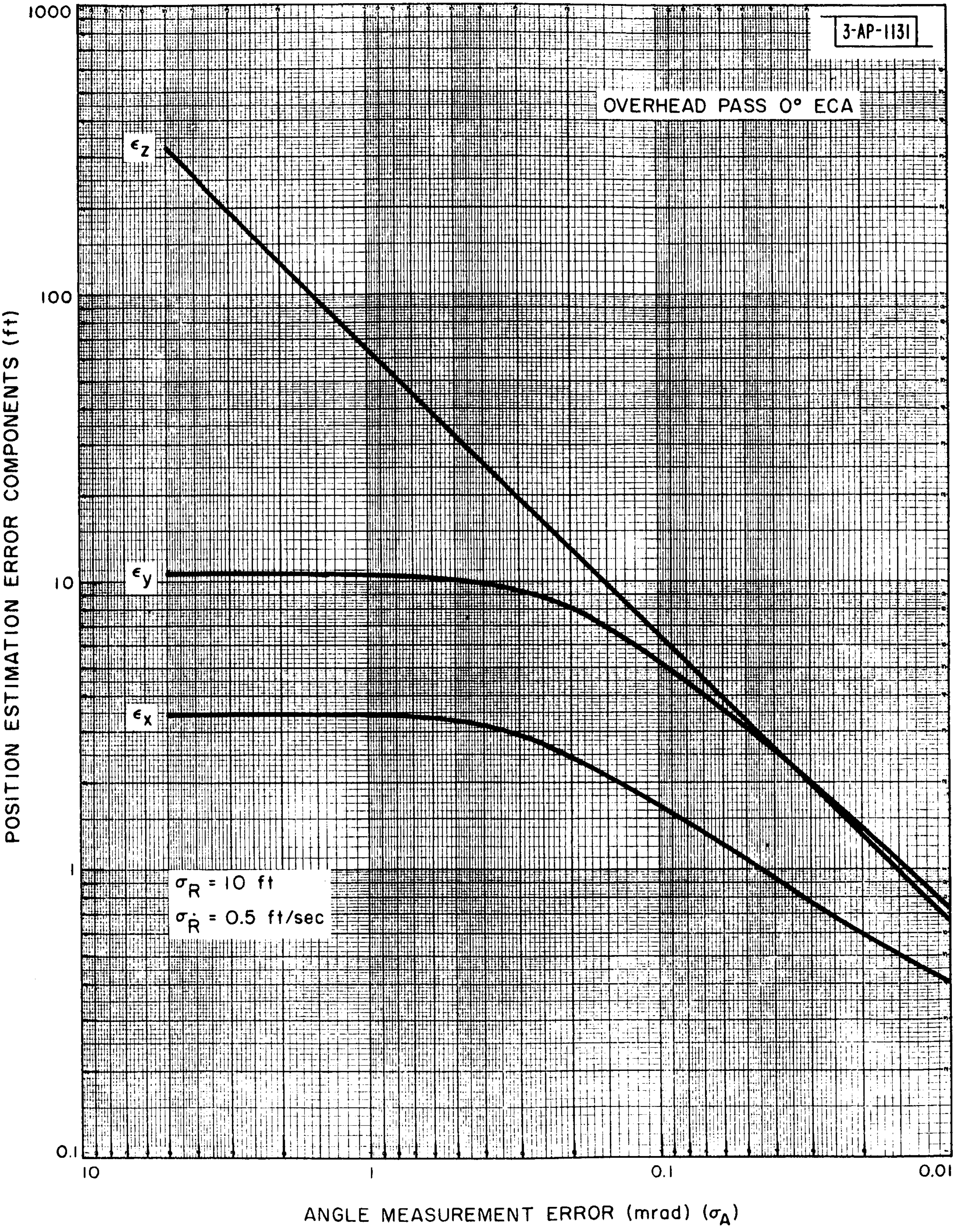

RADAR: 10 MEASUREMENTS/SECOND

NO *A PRIORI* INFORMATION

Figure A-13

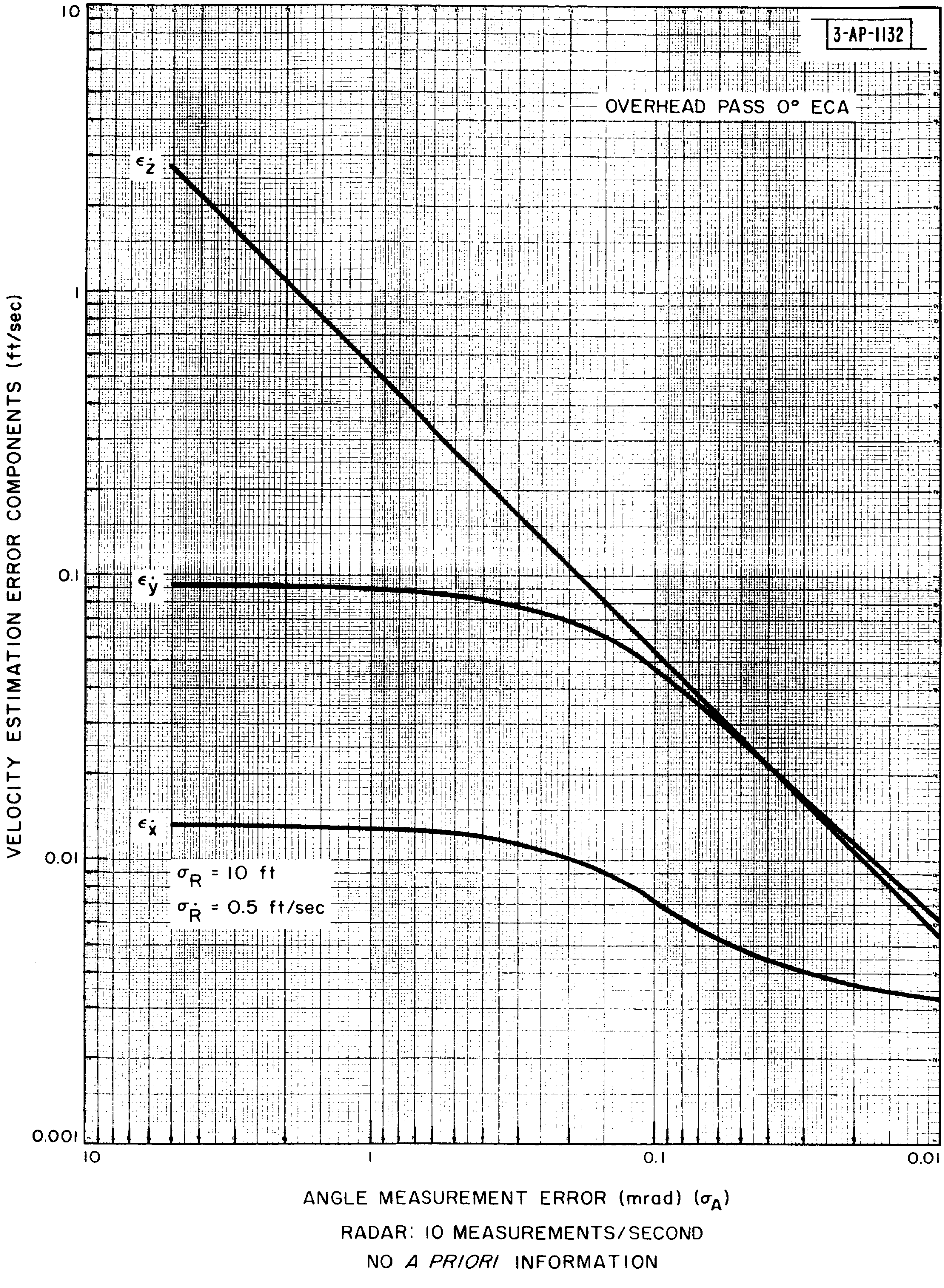
3-AP-1132
OVERHEAD PASS 0° ECA
$\epsilon_{\dot{z}}$
$\epsilon_{\dot{y}}$
$\epsilon_{\dot{x}}$
σ_R = 10 ft
$\sigma_{\dot{R}}$ = 0.5 ft/sec
10
1
0.1
0.01
0.001
VELOCITY ESTIMATION ERROR COMPONENTS (ft/sec)
ANGLE MEASUREMENT ERROR (mrad) (σ_A)
RADAR: 10 MEASUREMENTS/SECOND
NO *A PRIORI* INFORMATION

Figure A-14

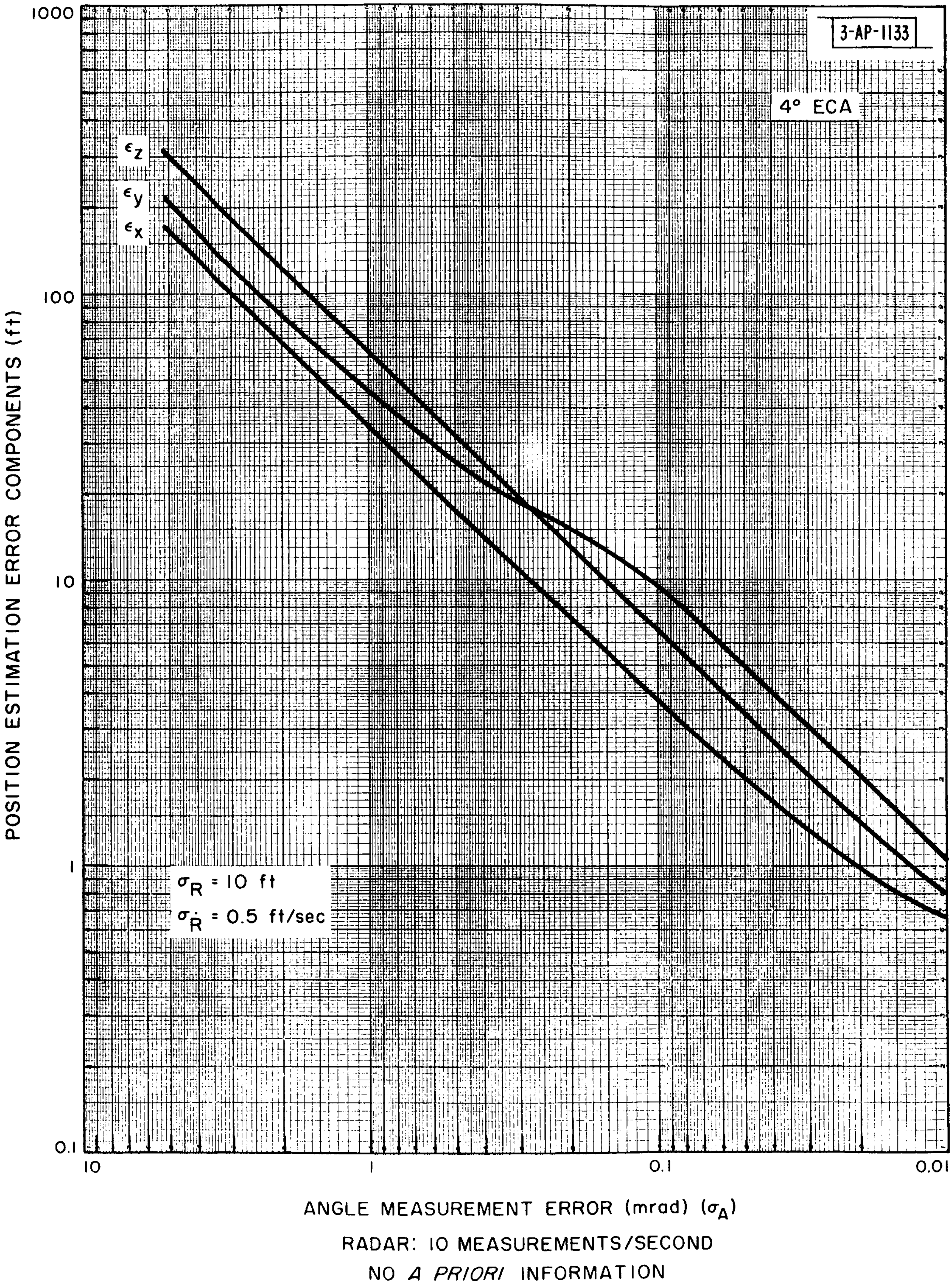

3-AP-1133
4° ECA
ϵ_z
ϵ_y
ϵ_x
σ_R = 10 ft
$\sigma_{\dot{R}}$ = 0.5 ft/sec
1000
100
10
1
0.1
POSITION ESTIMATION ERROR COMPONENTS (ft)
10
1
0.1
0.01
ANGLE MEASUREMENT ERROR (mrad) (σ_A)
RADAR: 10 MEASUREMENTS/SECOND
NO *A PRIORI* INFORMATION

Figure A-15

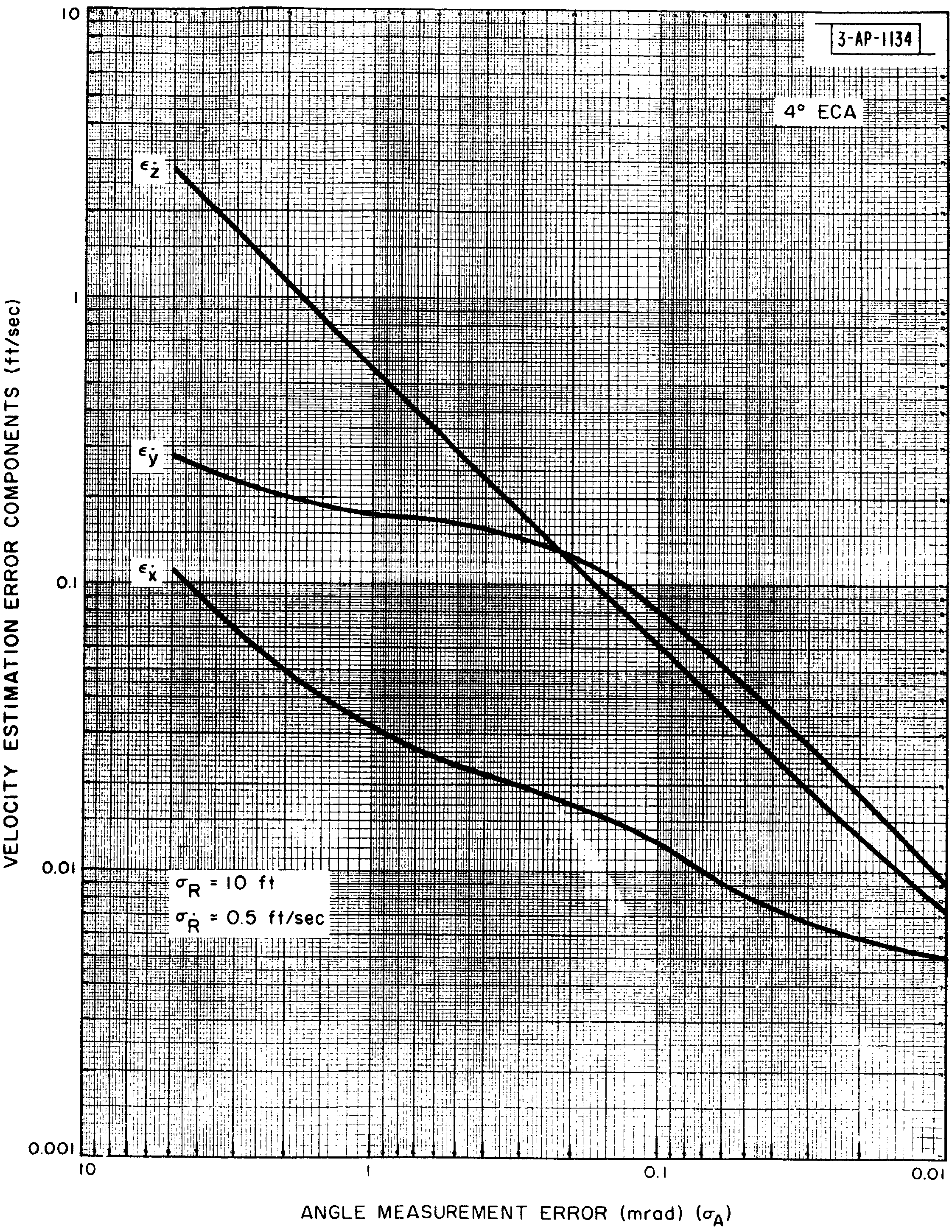

RADAR: 10 MEASUREMENTS/SECOND

NO *A PRIORI* INFORMATION

Figure A-16

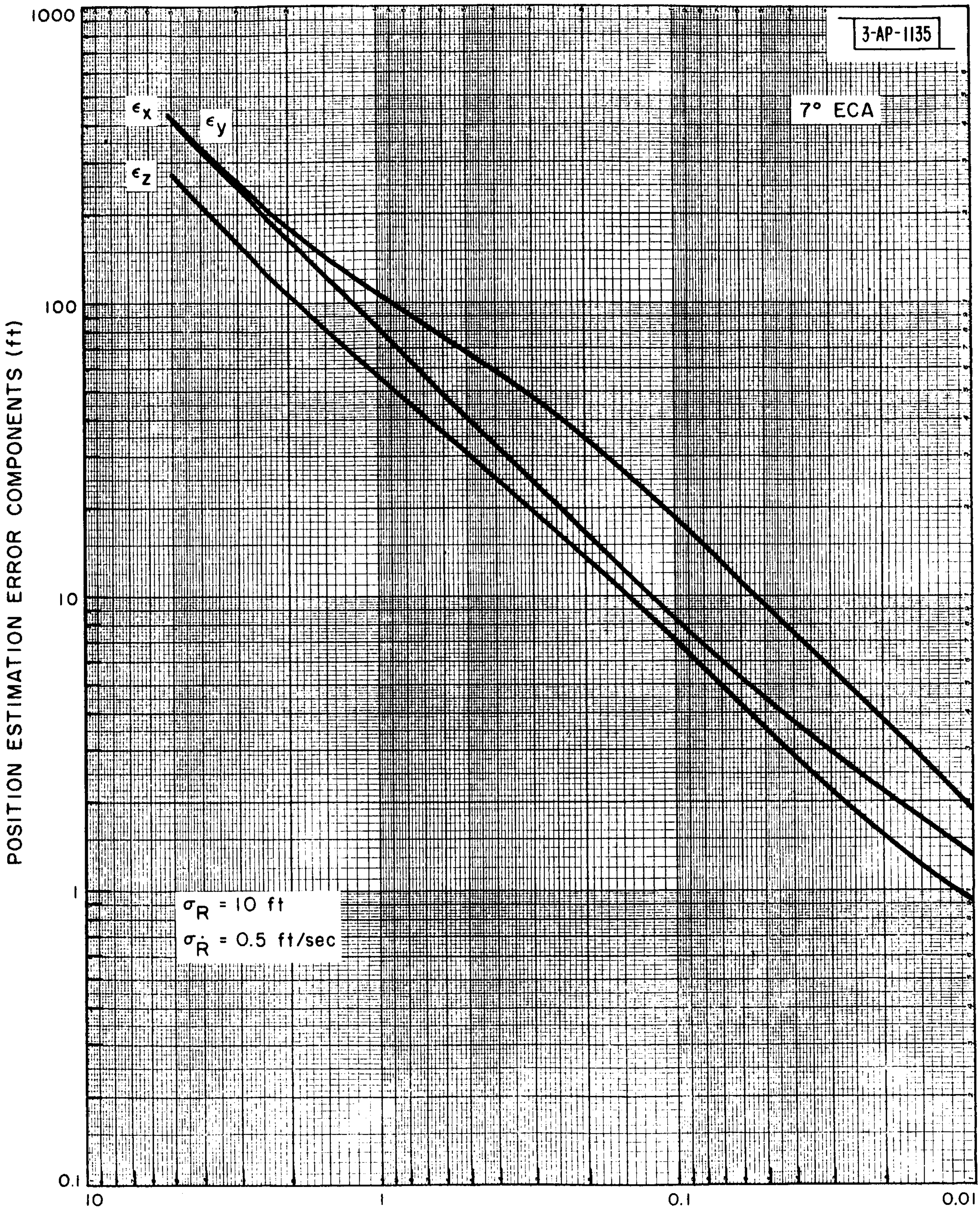

ANGLE MEASUREMENT ERROR (mrad) (σ_A)

RADAR: 10 MEASUREMENTS/SECOND

NO *A PRIORI* INFORMATION

Figure A-17

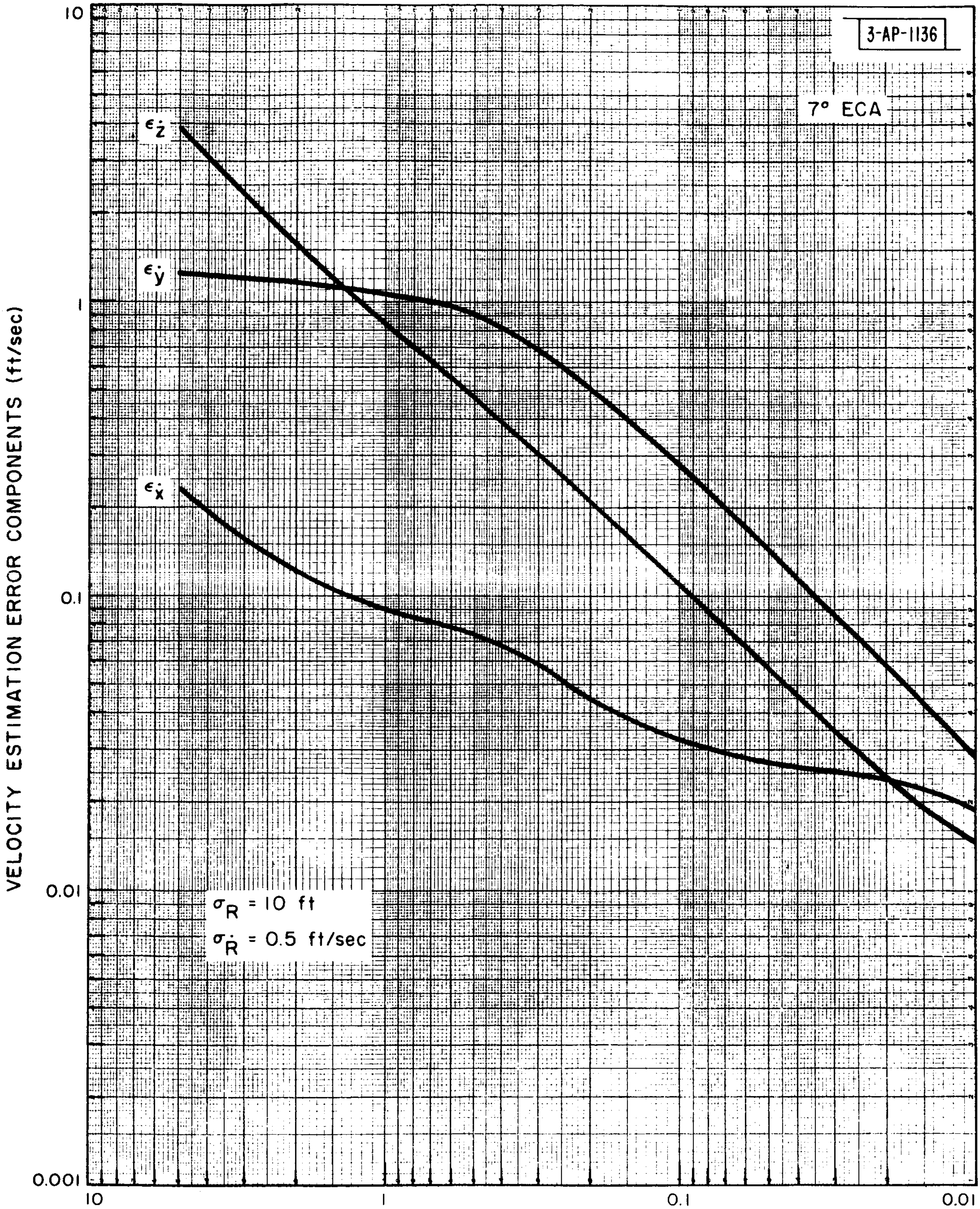

ANGLE MEASUREMENT ERROR (mrad) (σ_A)

RADAR: 10 MEASUREMENTS/SECOND

NO *A PRIORI* INFORMATION

Figure A-18

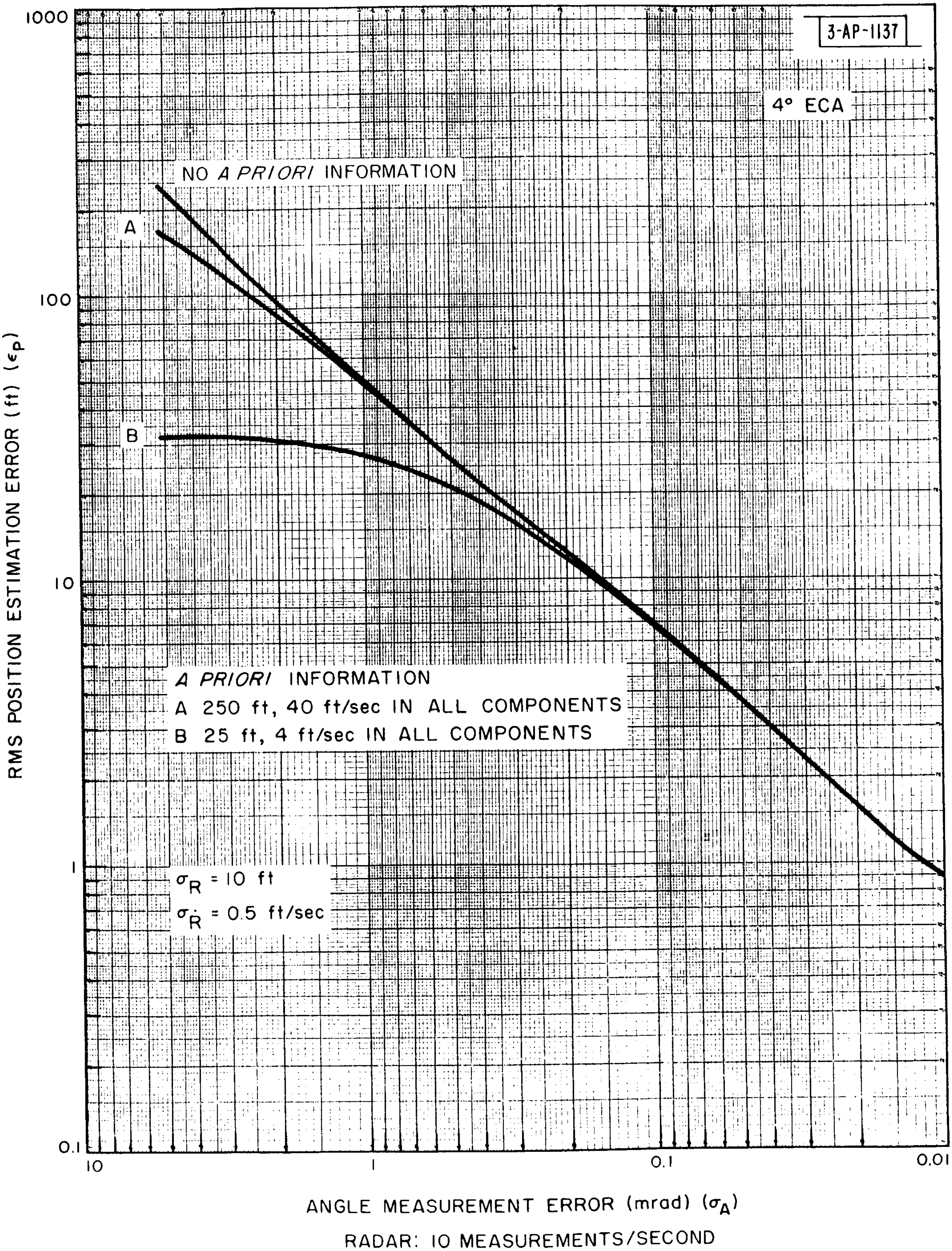
3-AP-1137
4° ECA
NO *A PRIORI* INFORMATION
A
B
A PRIORI INFORMATION
A 250 ft, 40 ft/sec IN ALL COMPONENTS
B 25 ft, 4 ft/sec IN ALL COMPONENTS
σ_R = 10 ft
$\sigma_{\dot{R}}$ = 0.5 ft/sec
RMS POSITION ESTIMATION ERROR (ft) (ϵ_p)
1000
100
10
1
0.1
10
1
0.1
0.01
ANGLE MEASUREMENT ERROR (mrad) (σ_A)
RADAR: 10 MEASUREMENTS/SECOND

Figure A-19

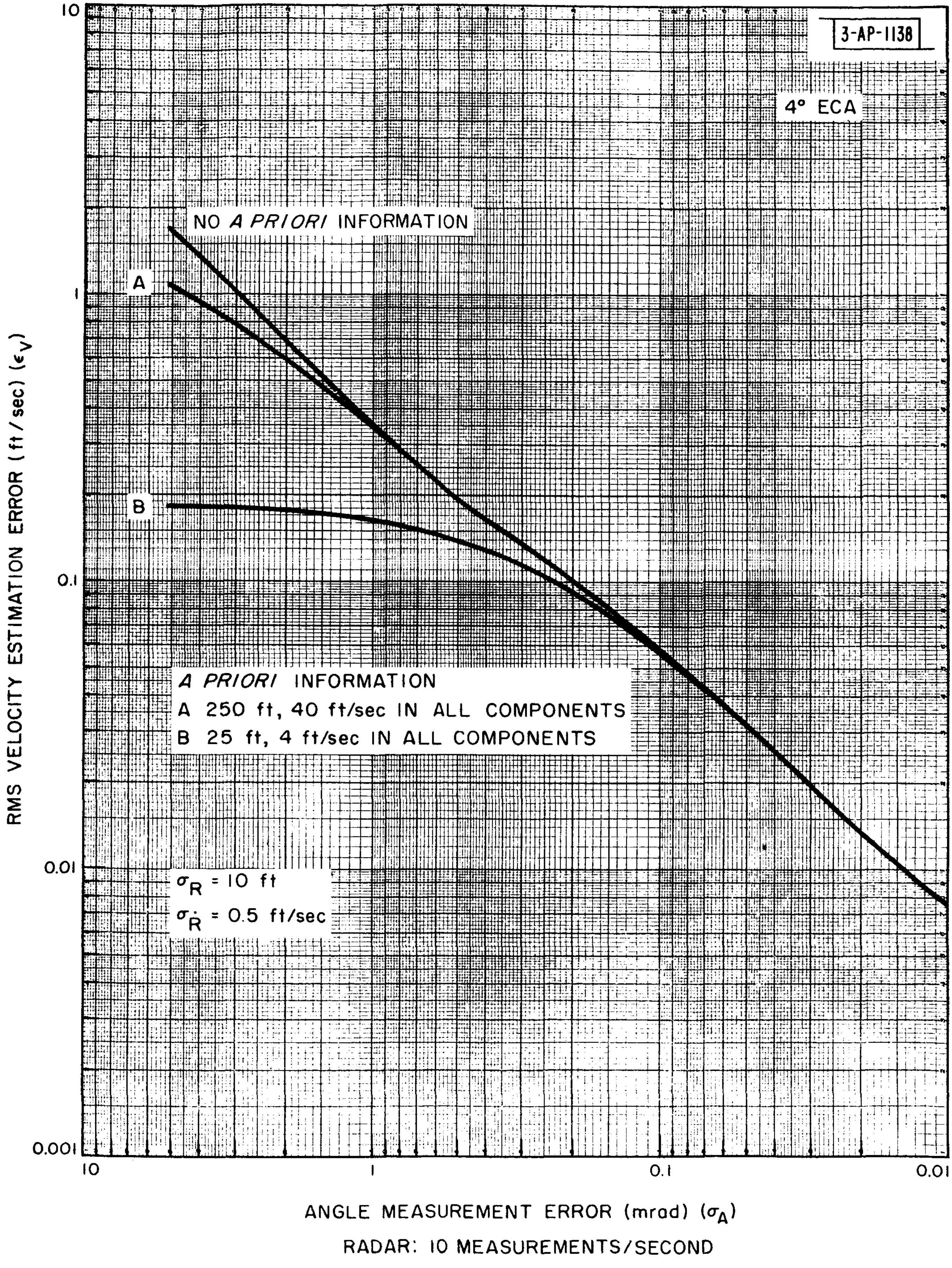
3-AP-1138
4° ECA
NO A PRIORI INFORMATION
A
B
A PRIORI INFORMATION
A 250 ft, 40 ft/sec IN ALL COMPONENTS
B 25 ft, 4 ft/sec IN ALL COMPONENTS
σ_R = 10 ft
$\sigma_{\dot{R}}$ = 0.5 ft/sec
RMS VELOCITY ESTIMATION ERROR (ft/sec) (ϵ_V)
10
1
0.1
0.01
0.001
10
1
0.1
0.01
ANGLE MEASUREMENT ERROR (mrad) (σ_A)
RADAR: 10 MEASUREMENTS/SECOND

Figure A-20

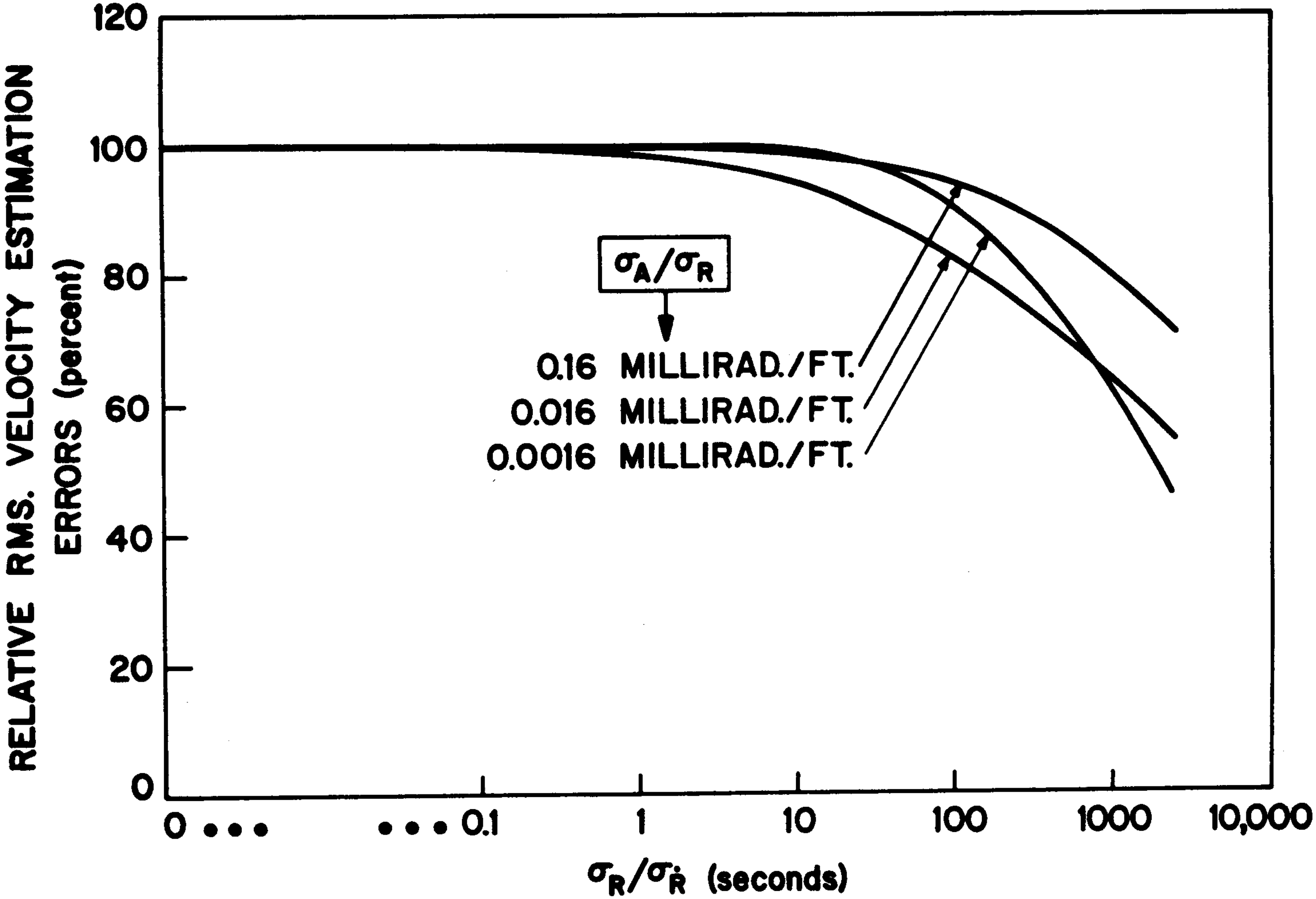

EFFECT OF RANGE-RATE ACCURACY

C28-81

Fig. A-21

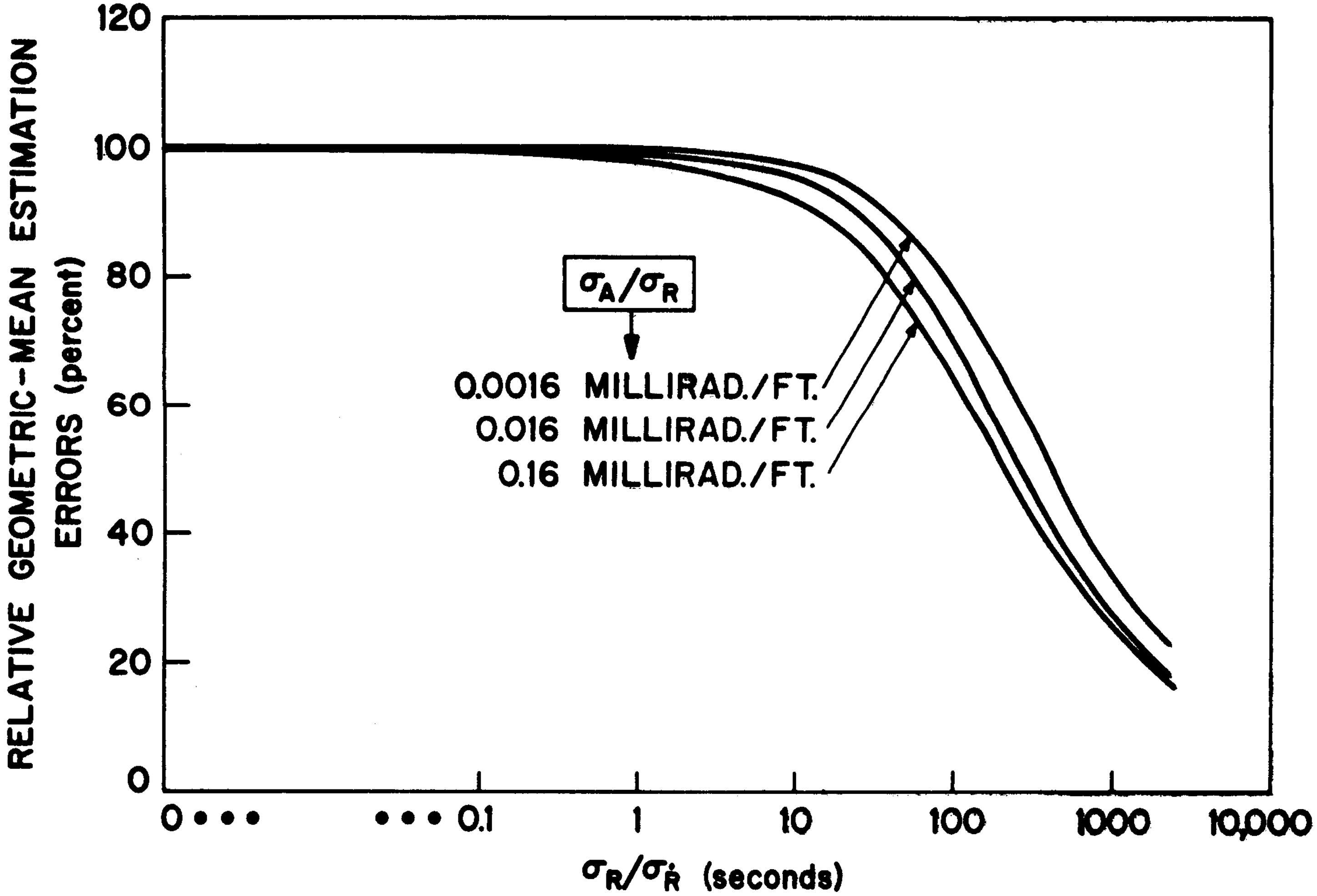

EFFECT OF RANGE-RATE ACCURACY

C28-80

Fig. A-22

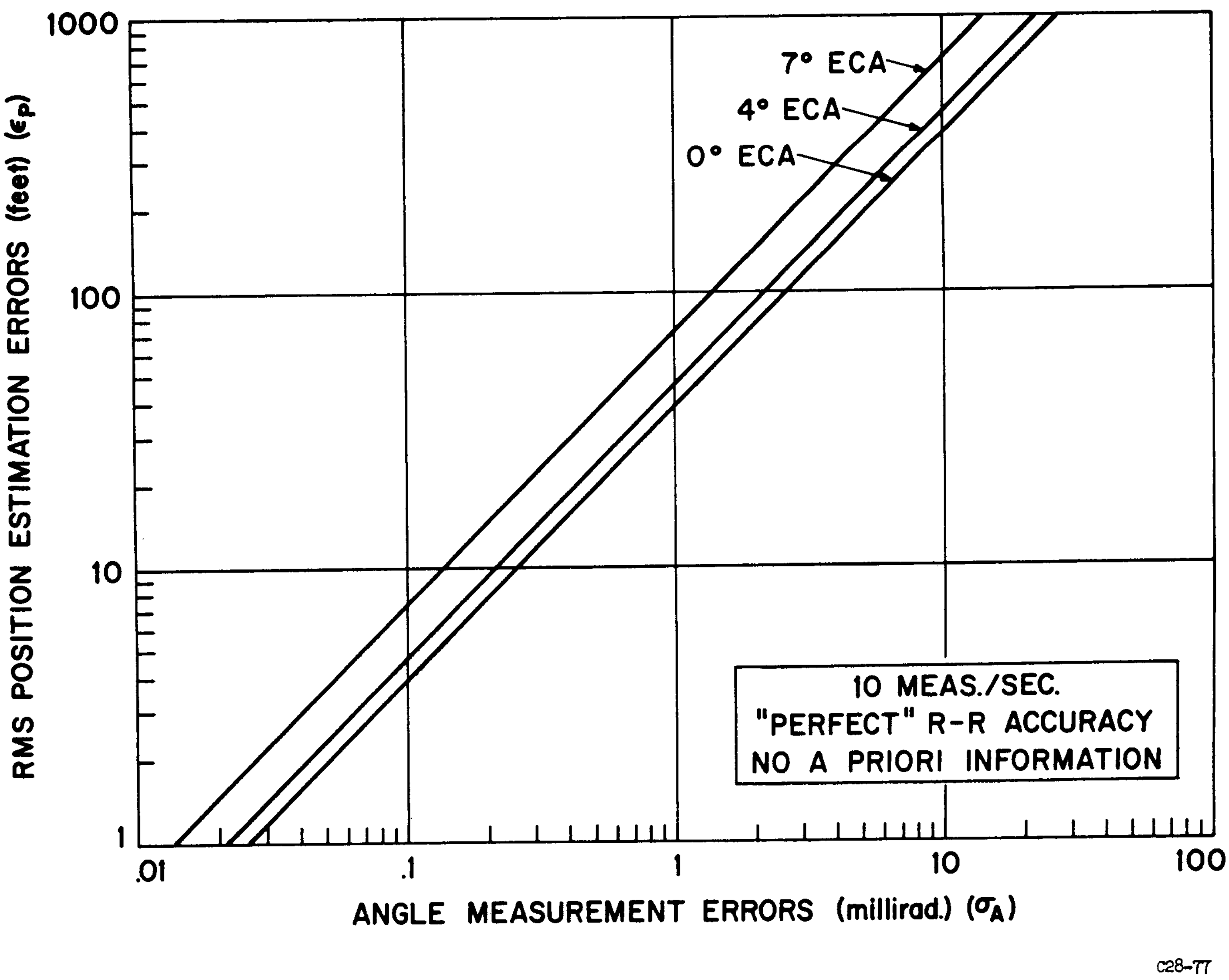
1000
100
10
1
.01
.1
1
10
100
RMS POSITION ESTIMATION ERRORS (feet) (ϵ_p)
ANGLE MEASUREMENT ERRORS (millirad.) (σ_A)
7° ECA
4° ECA
0° ECA
10 MEAS./SEC.
"PERFECT" R-R ACCURACY
NO A PRIORI INFORMATION
C28-77

Fig. A-23

DISTRIBUTION LIST

Director's Office

C. F. J. Overhage
W. H. Radford
H. W. Fitzpatrick
J. A. Kessler

Division 2

J. A. Arnow
F. Belvin
R. N. Davis
S. H. Dodd
R. G. Enticknap
O. V. Fortier
F. E. Heart
D. A. Koniver
M. S. Macrakis
A. J. Morency
B. J. Moriarty
H. C. Peterson
W. G. Schmidt
F. C. Schweppe
H. Sherman
J. Slesers
C. R. Wieser
D. Wiggert
Group 25 File

Division 4

J. G. Barry
J. A. Bosco
G. F. Dalrymple
J. C. Fielding
J. Freedman
B. S. Goldstein
W. F. Higgins
B. H. Labitt
W. W. Ward

Division 5

R. T. Mitchell

Division 7

J. F. Hutzenlaub

MIT, Instrumentation Laboratory

M. Trageser (2)

Jet Propulsion Laboratory
4800 Oak Grove Drive
Pasadena 3, California

P. Goodwin (2)
Telecommunications Division

J. J. Freeman Associates
8416 Georgia Avenue
Silver Spring, Maryland

Dr. J. J. Freeman

George C. Marshall Space Flight Center
Astrionics Division
Instrumentation Development Branch
Huntsville, Alabama

Mr. O. A. Hoberg

George C. Marshall Space Flight Center
Aeroballistics Division
Flight Evaluation Branch
Huntsville, Alabama

Dr. F. A. Speer

North American Aviation
Space and Information Systems Division
12214 Lakewood Boulevard
Downey, California

D. S. Levine (6)
NAA Sub-group 419-77

J. W. Small
Apollo Program Management Office, D/402

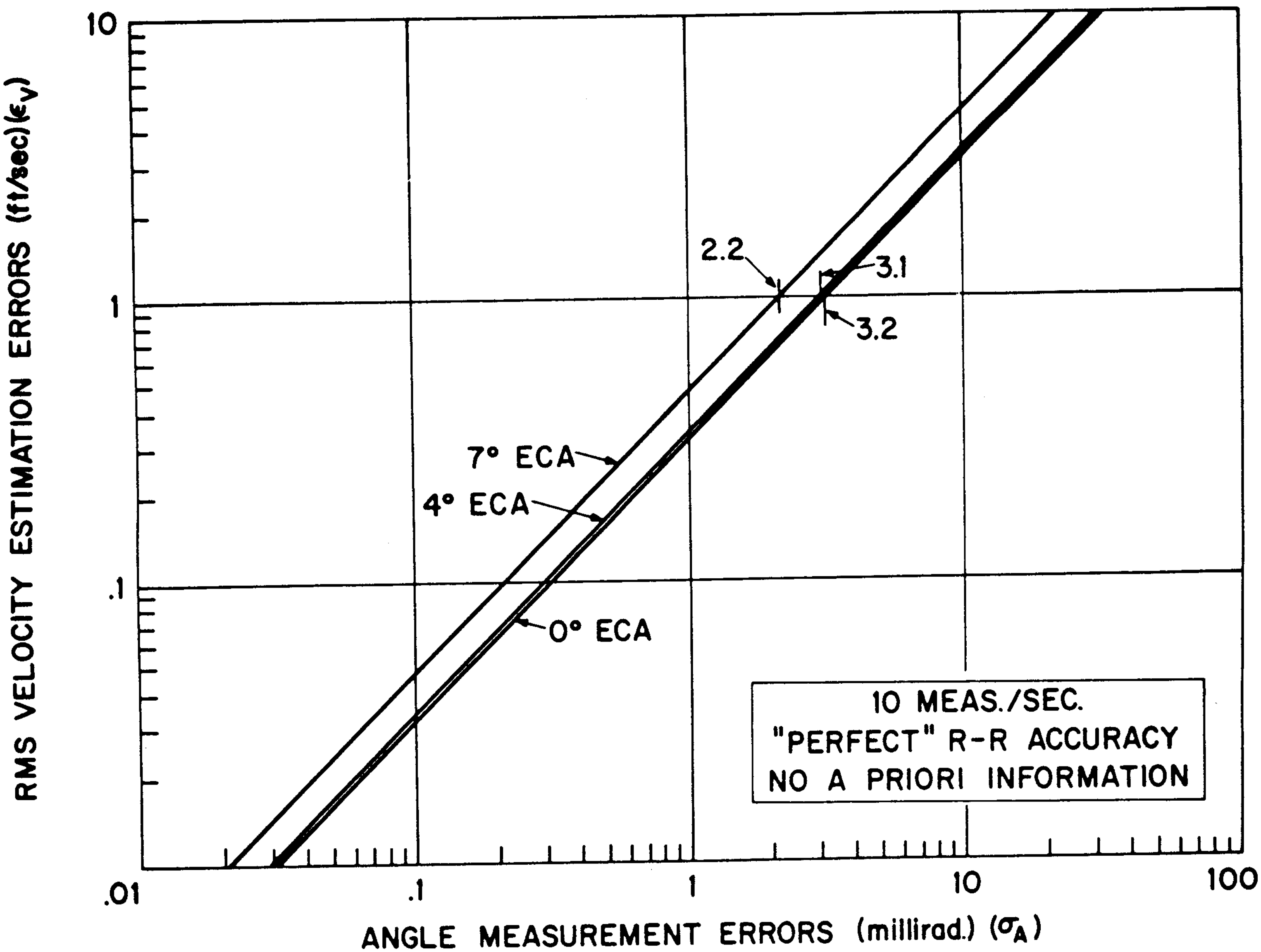

Fig. A-24

C28-78

M. Mullen, Librarian
Department 675-1, Mail Station 817
Philco Western Development Laboratory
3875 Fabian Way
Palo Alto, California

Goddard Space Flight Center
Greenbelt, Maryland

Dr. H. J. Goett, Director

Mr. J. T. Mengel, Ass't. Director
Tracking and Data Systems Directorate

Mr. C. A. Schroeder, Chief (8)
Tracking Systems Division

Dr. R. J. Coates, Assoc. Chief
Tracking Systems Division

Dr. F. O. Vonbun, Assoc. Chief
Tracking Systems Division

Dr. J. W. Siry, Chief
Theory and Analysis Staff
Tracking Systems Division

Dr. C. V. L. Smith, Chief (4)
Data Systems Division

Mr. F. J. Friel, Jr., Chief (4)
Operations Division

Mr. N. R. Heller, Chief (4)
Direct Data Division

Mr. O. Covington
Deputy Ass't. Director of Operations

NASA Headquarters (Attn: Code T)
400 Maryland Avenue, S. W.
Washington 25, D. C.

R. D. Briskman
C. R. Morrison

NASA - Langley Research Center
Hampton, Virginia

C. J. Donlon (2)
J. E. Stitt

Scientific and Technical Information Facility (2)
Attn: NASA Representative (S-AK/RKT)
P. O. Box 5700
Bethesda, Maryland

NASA - Manned Spacecraft Center
P. O. Box 1536
Houston, Texas

Apollo Project Office
D. R. Broome
E. L. Chicoine
D. Fielder (5)
M. R. Franklin
D. W. Gilbert
J. Heberlig (2)
M. Jenkins
H. C. Kyle
MSC Files (3)
H. E. Meily (Lincoln Lab. Representative)
L. E. Packham
R. O. Piland
J. A. Roberts
R. Sawyer
T. Skopinski
W. Williams

NASA - Flight Research Center
Box 273
Edwards, California

K. C. Sanderson
FRC Files

NASA - Pre-Launch Operations
Hangar S
Cape Canaveral, Florida

J. Moser
J. Williams